NEUTRON DAMAGED GE(LI) GAMMA RAY DETECTORS

THE CHANGE IN THE RESPONSE OF GE(LI) RADIATION DETECTORS DUE TO DAMAGE CAUSED BY HIGH ENERGY NEUTRONS

By

ROGER GEORGE CLAUS, B.Sc.,B.Ed.

A Thesis

Submitted to the Faculty of Graduate Studies

in Partial Fulfilment of the Requirements

for the Degree

Master of Science

McMaster University

September 1970

MASTER OF SCIENCE (1970) McMASTER UNIVERSITY
(Physics) Hamilton , Ontario.

TITLE: The Change in the Response of Ge(Li) Gamma Radiation Due to Damage Caused by High Energy Neutrons

AUTHOR: Roger George Claus, B.Sc. (McMaster University)
B.Ed. (University of Toronto)

SUPERVISOR: Dr. T. J. Kennett

NUMBER OF PAGES: vii, 62

SCOPE AND CONTENTS:

This thesis deals with the changes, in the response of a Ge(Li) gamma ray detector, arising from damage caused by its exposure to high energy neutrons. The phenomenon of charge trapping is considered and included in a model explaining the collection of electron-hole pairs in a Ge(Li) detector. From this model a response function for the output of the detector is obtained and then applied to a description of the changes in FWHM of pulse height spectra peaks with energy and neutron irradiation.

Described are experiments in which three detectors were exposed to fast neutrons and their changing response was related to the response function. Finally the number of damage centres produced by the neutrons is discussed.

ACKNOWLEDGEMENTS

I wish to express my appreciation to those to whom I owe a debt for their encouragement, suggestions and helpful discussions. In particular, I feel special gratitude to my research director, Dr. T. J. Kennett, without whose help I would not have finished this project. To Mr. L. C. Henry I owe a great deal for his help in carrying out experiments.

TABLE OF CONTENTS

		Page
CHAPTER I	INTRODUCTION	1
CHAPTER II	THEORY OF CHARGE COLLECTION AND TRAPPING IN GE(LI) DETECTORS	4
	2.1 Intrinsic Semiconductor	4
	2.2 Extrinsic Semiconductor	6
	2.3 P N Junction as a Detector	7
	2.4 Radiation Damage in Semiconductor Detectors	9
	2.5 Charge Collection	10
	2.6 Width of Pulse Height Peaks	21
CHAPTER III	EXPERIMENTAL ARRANGEMENT	23
	3.1 Introduction	23
	3.2 Irradiation of Planar Detectors	24
CHAPTER IV	IRRADIATION EFFECTS	32
	4.1 Planar Detector "A"	32
	4.2 Planar Detector "B"	43
	4.3 Single Open-Ended Coaxial Detector	51
	4.4 Summary	57
REFERENCES		60

LIST OF FIGURES

Figure No.	Title	Page
1	(a) The formation of a forbidden band gap in germanium. (b) Energy diagram of conduction band and balence band. (c) The same levels as in (b), the addition of donor and acceptor levels.	5
2	Ideal detector.	11
3	Variation of ξ across the width of the intrinsic region for different β.	15
4	Response function $P(\xi)$ with different β.	19
5	Vacuum chamber for irradiating detectors.	26
6	Collimated gamma-ray source	28
7	Top: Ratio of peak height to peak area against position of collimated source for detector A before irradiation. Bottom: Skewness against position of collimated source for detector A before irradiation.	33
8	Pulse height peak response of counter to 2614 keV gamma rays for 0 neutrons, 3.2×10^8 neutrons, 14.4×10^8 neutrons and 21.8×10^8 neutrons	35
9	Skewness, Δ, for different energies at 0 neutrons, 3.2×10^8 neutrons, 14.4×10^8 neutrons and 21.8×10^8 neutrons.	38
10	Average skewness measured during irradiation.	40
11	Variation of FWHM of detector A and analyzing system during irradiation for various energies.	42
12	Top; Ratio of peak height to peak area against collimated source position for detector A after irradiation.	44

Figure No.		Title	Page
	Bottom:	Skewness against collimated source position for detector A after irradiation.	
13	Top:	Ratio of peak height to peak area against collimated source position for counter B before irradiation.	45
	Bottom:	Skewness against collimated source position for counter B before irradiation.	
14		Variation of FWHM of detector band analyzing system during irradiation for different gamma ray energies.	49
15	Top:	Ratio of peak height to peak area against collimated source position for counter B after irradiating.	50
	Bottom:	Skewness against collimated source position for counter B after irradiation.	
16		Correlation of normalized skewness measured during irradiation against gamma ray energy.	53
17		Average skewness measured at different times during irradiation.	56
18		Variation of FWHM of single open ended co-axial detector and analyzing system during irradiation for different gamma ray energies.	58

LIST OF TABLES

Table No.	Title	Page
I	Skewness at different energies during irradiation	36
II	Average skewness during irradiation	39
III	Skewness measured before irradiation	47
IV	Skewness measured after irradiation.	47
V	Skewness at different energies during irradiation	54
VI	Skewness normalized to $\bar{\Delta}$ during irradiation	55

CHAPTER I

INTRODUCTION

In the experimental application of Ge(Li) gamma ray detectors, a fast neutron background is sometimes present. The nuclear interaction of the neutrons with the germanium atoms of the counter produce characteristic radiation which can be observed in the spectrum and which indicate the presence of the damage process. This radiation has been documented by other experimentation[1]. In addition to producing unwanted background, the fast neutrons have a detrimental effect on the performance of the unit and its useful life can be drastically reduced. Radiation damage of Ge(Li) counters has been investigated previously for various neutron energies[2]. The reported effects on gamma ray detectors have been to increase the leakage current, to lower detector capacitance, to degrade the rise time and pulse height resolution and to distort the shape of the pulse height peaks. It has also been proposed in the same work that damage from fast neutrons takes the form of atomic displacement from the lattice. These dislocations serve as trapping centres predominantly for hole type carriers. They delay the collection of charges by the electric field for a time longer than the time constants of the subsequent

analysing system. This effectively removes these charges from the detector signal, thus presenting an incomplete signal for analysis.

It is also evident that the amount of trapping of the carriers would depend on the distance to be traversed by them through the semiconductor. Since gamma ray interactions cannot be confined to a localized point within the detector, it follows that there would be a variation in the relative number of charged particles collected and included in the detector signal. This would affect the timing resolution and distort the pulse height peak shape.

These earlier investigations leave unanswered several questions about fast neutron damage. The relationship between carrier lifetime in Ge(Li) detectors and the integrated neutron flux is yet to be found. The functional dependence of the shape of pulse height peaks on the total neutron dose is unknown. One last question concerns the response of the counter to gamma ray energies beyond 1 MeV, for increasing neutron exposure, for which no work has been reported.

In an effort to answer these questions, experiments were undertaken using three different detectors. Two of these were planar counters and the other was of the five sided coaxial configuration. One planar device and the coaxial counter were both fabricated[3] out of Hoboken supplied germanium.

The other planar detector was supplied by Sylvania. The response of the two planar detectors were measured for gamma rays of energies up to about 2.6 MeV. The five sided coaxial counter was involved in a long term experiment with a collimated gamma ray beam that was contaminated with fast neutrons. The gamma ray spectrum covered an energy range up to 10.5 MeV. and data were taken continuously for a period of over a month. In this time the counter was exposed to about 0.6×10^{10} neutrons. Thus a well documented history of radiation damage was provided from this experiment.

In order to account for carrier trapping in a semiconductor gamma-ray detector, a mathematical model is proposed and tested against the measurements made on these counters. From this, a description of the change, with increasing damage, in the resolution of a Ge(Li) spectrometer system is provided.

CHAPTER II

THEORY OF CHARGE COLLECTION AND TRAPPING IN GE(LI) DETECTORS

Since the trapping effects of carriers depends on the conduction characteristics of the semiconductor involved, it is worthwhile to review the theory of operation of semiconductor detectors.

2.1 Intrinsic Semiconductor

Consider a number, N, of germanium atoms that assembled to form a single crystal. As the interatomic spacing decreases, as shown in Figure (1), the 4s and 4p atomic levels broaden into energy bands which first overlap and then split into two components. At the equilibrium spacing, a, the two energy bands are separated by about 0.68 eV and each contain 4n states. The lower band is known as the valence band, for there are 4n valence electrons available to exactly fill it. Physically, the valence band represents the states of all the electrons which make up the covalent bonds between the atoms. These electrons are normally engaged in the bonds and are not available for conduction purposes.

If an electron acquires at least 0.68 eV of energy it leaves the valence band and populates the conduction band, where it is free to migrate throughout the crystal. In physical terms it could be said that the electron is removed

FIGURE 1

(a) The formation of a forbidden band gap in germanium.

(b) Energy diagram of conduction band and balance band.

(c) The same levels as in (b), the addition of donor and acceptor levels.

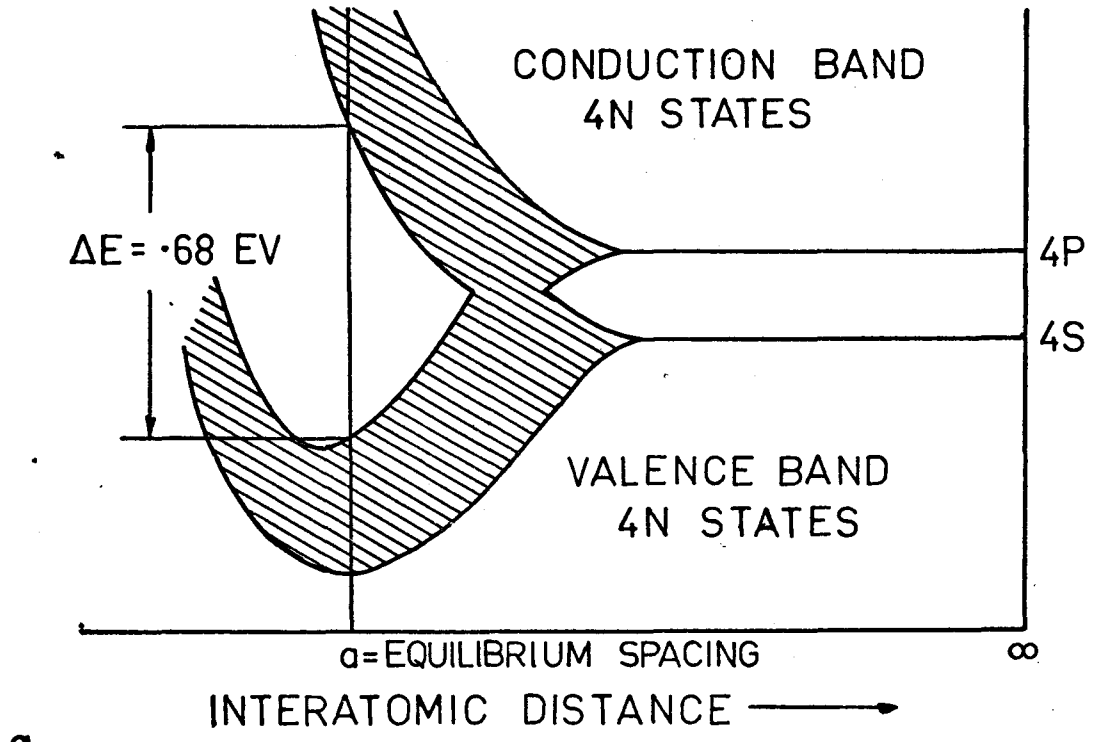
CONDUCTION BAND
4N STATES
ΔE = ·68 EV
4P
4S
VALENCE BAND
4N STATES
a=EQUILIBRIUM SPACING
∞
INTERATOMIC DISTANCE

a

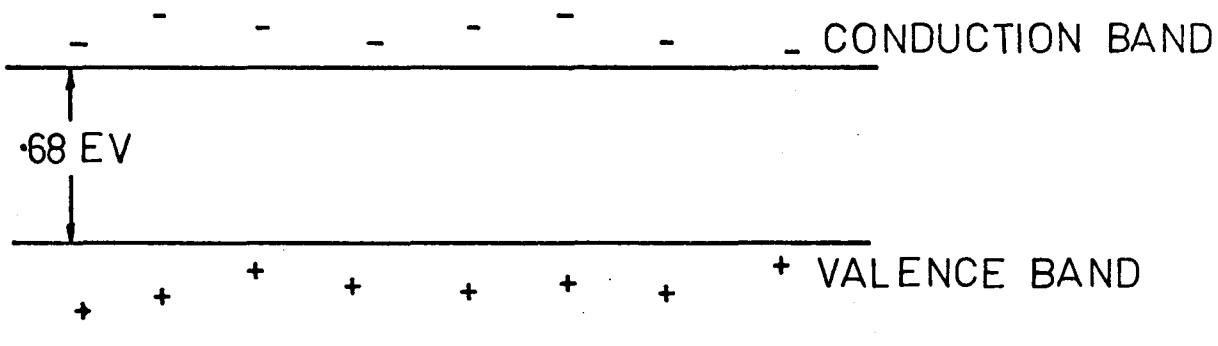
CONDUCTION BAND
·68 EV
VALENCE BAND

b

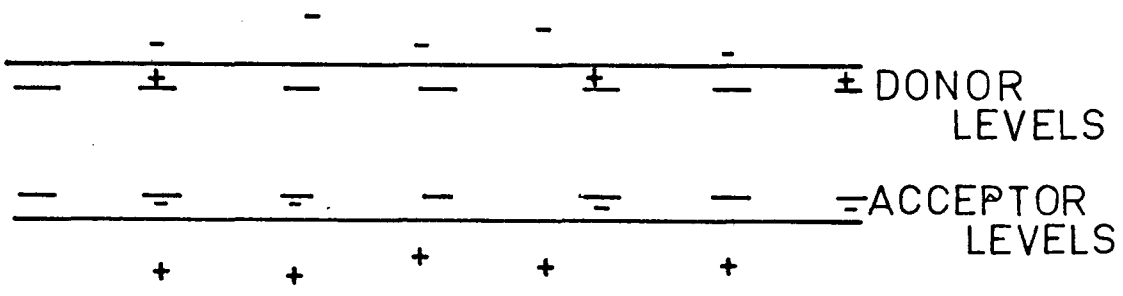
DONOR
LEVELS
ACCEPTOR
LEVELS

c

FIG. 1

from the covalent bond and moves randomly throughout the crystal under the influence of the thermal agitation of the lattice. Likewise the vacancy left by the electron, also known as a hole, is free to migrate since an electron in a covalent bond adjacent to the hole may move into it, thus transferring the hole to the electron's former location. Under the influence of an electric field the electrons would migrate toward the positive electrode while the holes would tend toward the negative electrode, thus producing a macroscopic electric current.

It is seen that for every free electron there is a positive hole and that both were created only by thermal excitation of electrons across the band gap. This forms an intrinsic semiconductor and the holes and electrons are called intrinsic charge carriers.

2.2 Extrinsic Semiconductor

If, in the formation of the crystal, small amounts of either some group III element or some group V element were included so that one of these atoms were substituted for a germanium atom, an impurity semiconductor results. If a group III impurity was included, there would be only three valence electrons to form covalent bonds with its neighbour. A hole would be left in place of the fourth bond. A semiconductor in which a majority of the carriers are holes results and this crystal is called a p-type

semiconductor.

Likewise, if a group V atom were substituted for a germanium atom in the lattice, four electrons would be engaged in covalent bonds while the fifth would be vound in a relatively weak fashion. Under thermal agitation, this atom is easily ionized thus providing an extra electron for conduction purposes. This type of crystal is called an n-type semiconductor since a majority of the carriers are electrons.

This picture would be represented in the band model as isolated levels introduced in the forbidden energy band gap by the impurities as shown in Figure (1). For n-type semiconductors, donor atoms would introduce donor levels in the upper part of the gap very close to the conduction band. Thus little energy is required to raise the electrons to the conduction band and to provide an excess of electrons as the principle charge carrier. Likewise for p-type semiconductors, acceptor atoms would introduce acceptor levels in the lower part of the band gap close to the valence band. Again, electrons from the valence band would require very little energy to transfer to the acceptor levels, leaving an abundance of holes in the valence band as charge carriers.

2.3 P N Junction as a Detector

Consider a P type semiconductor placed together with an N type semiconductor. The transition region between the

two forms a junction in which electrons from the region move into the P region to compensate the holes and likewise, holes from the P region move into the N region. This process sets up a net positive charge in the N region and a net negative charge in the P region each of which then opposes the movement of carriers. Thus a potential barrier to the movement of charge carriers existing across the P N junction maintains an equilibrium condition with the concentration of holes and electrons. The application of a reverse bias across the junction, that is an external voltage is applied across it with the negative charge being attached to the P region, increases the potential barrier by repelling with greater force, electrons from the N region and attracting holes in the P region.

If holes and electrons, however, are formed within the junction region by thermal excitation or by other means then the electric field would sweep the holes toward the P region and the electrons toward the N region, each with a velocity depending on their mobility. This would give rise to a current pulse in the external circuit. The introduction of a charged particle to the junction region would energize electrons sufficiently to produce a number of electron hole pairs proportional to its energy. In fact in germanium a particle with an energy of 2.98 ± 0.1 eV of energy is required to produce one electron hole pair[4].

Gamma rays interacting with the atoms in the junction produce Compton electrons and photo electrons which would in turn produce electron-hole pairs which could again be detected with external circuits. Thus the P N junction operates as a gamma ray detector.

In Ge(Li) detectors, compensation over a large volume is accomplished by using lithium as an interstitial impurity in gallium-doped germanium. Since lithium ionizes easily, it compensates the gallium acceptors to form a large volume intrinsic region in which the charge carriers are composed of equal numbers of electrons and holes. A reverse bias across this PIN junction operates in the same way as for a normal P N junction in sweeping out electron hole pairs produced by ionizing radiation. Thus a Ge(Li) detector forms a capable large volume gamma ray detector.

2.4 Radiation Damage in Semiconductor Detectors

The primary effect of fast neutron irradiation of a Ge(Li) detector is the displacement of atoms from the lattice. If a neutron collides either elastically or inelastically with a germanium atom it may be knocked from its lattice site in the subsequent recoil and still retain considerable energy. This energy is expended in collisions with other atoms, removing them from the lattice as well, before coming to rest. The result is a number of pairs of

empty lattice sites and interstitial germanium atoms, or Frenkel defects. It has been estimated[2] that for a 1.1 MeV neutron incident on a Ge(Li) detector, about 130 such defects are produced. These lattice imperfections act either as electron traps or as hole traps. Charge carriers encountering such a trap while being swept out of the intrinsic region are temporarily removed or trapped by the defect for a time T. If T is longer than the integration time constants of the external amplifier then the contribution of that carrier to the external signal is removed. In addition it was found[2] that the result of damage was to trap preferentially, trapping either holes or electrons so that the loss of one type of carrier contributed to the degeneration of the signal. It is seen then that the occurrence of damage due to fast neutron irradiation results in a degradation of the detector performance. In the next section a model of this is formulated.

2.5 Charge Collection

On the basis of the preceding information the processes of charge collection in a semiconductor detector can be formulated. Consider first an ideal counter, Figure (2), of the planar configuration, in which the applied electric field, E, is constant everywhere and trapping effects are insignificant. The electrode separation in this counter

FIGURE 2

Ideal detector

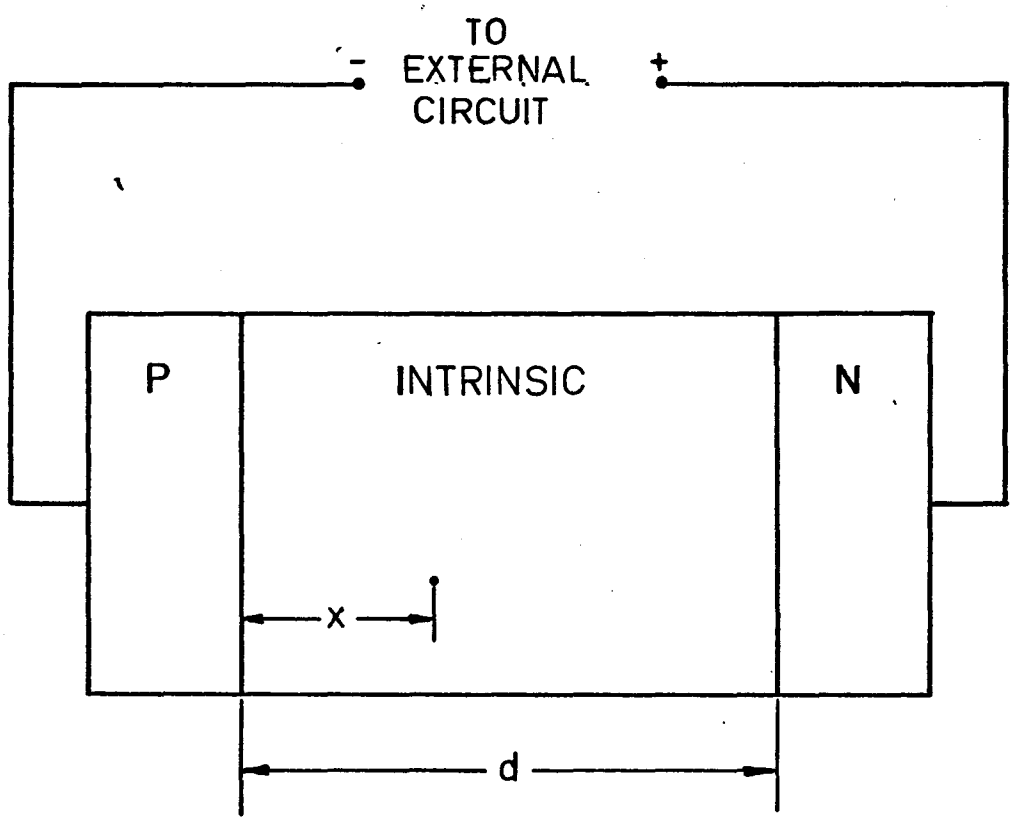

FIG. 2 : IDEAL DETECTOR

is d. A charged particle is incident on the counter and in coming to rest, it generates a number, say N, hole-electron pairs at a distance x from the negative electrode. The signal produced in the external circuit is of two components, that from the collection of holes and that from the collection of electrons. First the holes moving to the negative electrode give rise to a current flow of:

$$i_h = Nev_h \qquad (1)$$

The integrated charge measured in the external circuit is then:

$$Q_h = \int_0^{t=\frac{x}{vh}} Nev_h dt$$

$$= Nex \ . \qquad (2)$$

For the electrons being collected over a distance d-x in a time $\frac{d-x}{V_e}$ the corresponding charge seen in the external circuit is:

$$Q_e = Ne(d-x) \qquad (3)$$

Thus the total signal that is measured is:

$$Q = Q_h + Q_e = Ned \qquad (4)$$

Consider now the existence of trapping centres which serve to trap to a significant extent only one type of charge carrier, say holes. In this analysis the result is the same if electrons are trapped instead, since we shall

assume both holes and electrons have the same mobility. It is assumed that the time spent by a hole in a trap is much longer than the collection time of untrapped charges, that is, no significant detrapping occurs. The number of holes as a function of time considered independently of charge collection is then:

$$N_h(t) = N_h e^{-t/\tau} \tag{5}$$

where τ is the normal relaxation lifetime for holes in the counter. Then the current due only to collected holes would be:

$$i = Ne^{-t/\tau}\, ev_h \tag{6}$$

and the charge seen in the external circuit would be:

$$Q_h = \int_0^{t=\frac{x}{v}} Ne^{-t/\tau}\, ev_h dt$$

$$= Ne\, v_h\, \tau\left(1 - e^{-\frac{x}{v_h \tau}}\right) . \tag{7}$$

For simplification, let $\alpha = \frac{x}{d}$ and $\beta = \frac{\tau}{t_o}$ (where t_o is the maximum collection time) be the normalized variables for position and lifetime. The expression for the charge collected due to holes then becomes:

$$Q_h = N_{ed}\beta(1 - e^{-\alpha/\beta}) \tag{8}$$

and for the relatively untrapped electrons:

$$Q_e = N_{ed}(1 - \alpha) . \tag{9}$$

Therefore the total signal from both electrons and holes is just:

$$Q_e = N_{ed}(1 - \alpha + \beta(1 - e^{-\alpha/\beta})) \qquad (10)$$

Expressing equation (10) as a normalized charge the result is:

$$\xi = (1 - \alpha + \beta(1 - \exp(-\alpha/\beta)). \qquad (11)$$

It can be seen that for an ideal counter the detector signal is independent of the position at which the charge pairs are formed. The lifetime of the carriers is infinitely long so that this parameter does not enter into the equation. If preferential trapping occurs in a time τ, however, the total signal is not independent of the position where the carriers were formed or of the carrier lifetime. To illustrate this Figure (3) shows the values of the normalized charge $\xi = \frac{Q}{Ned}$ for $0 \leq \alpha \leq 1$ and various β from 10^{-2} to 10^{3}.

When $\alpha = 0$, this corresponds to events occurring at the negative electrode and hence insignificant trapping of carriers since all of the contributions to ξ come from the electron collection. When $\alpha = 1$, corresponding to initial carrier production at the positive electrode, trapping occurs and is dependent on the value of β. For very large values of β, $\xi \simeq 1$ for all α indicating ideal conditions are approached when the lifetime of the carriers is much larger than the collection time.

FIGURE 3

Variation of ξ across the width of the intrinsic region for different β.

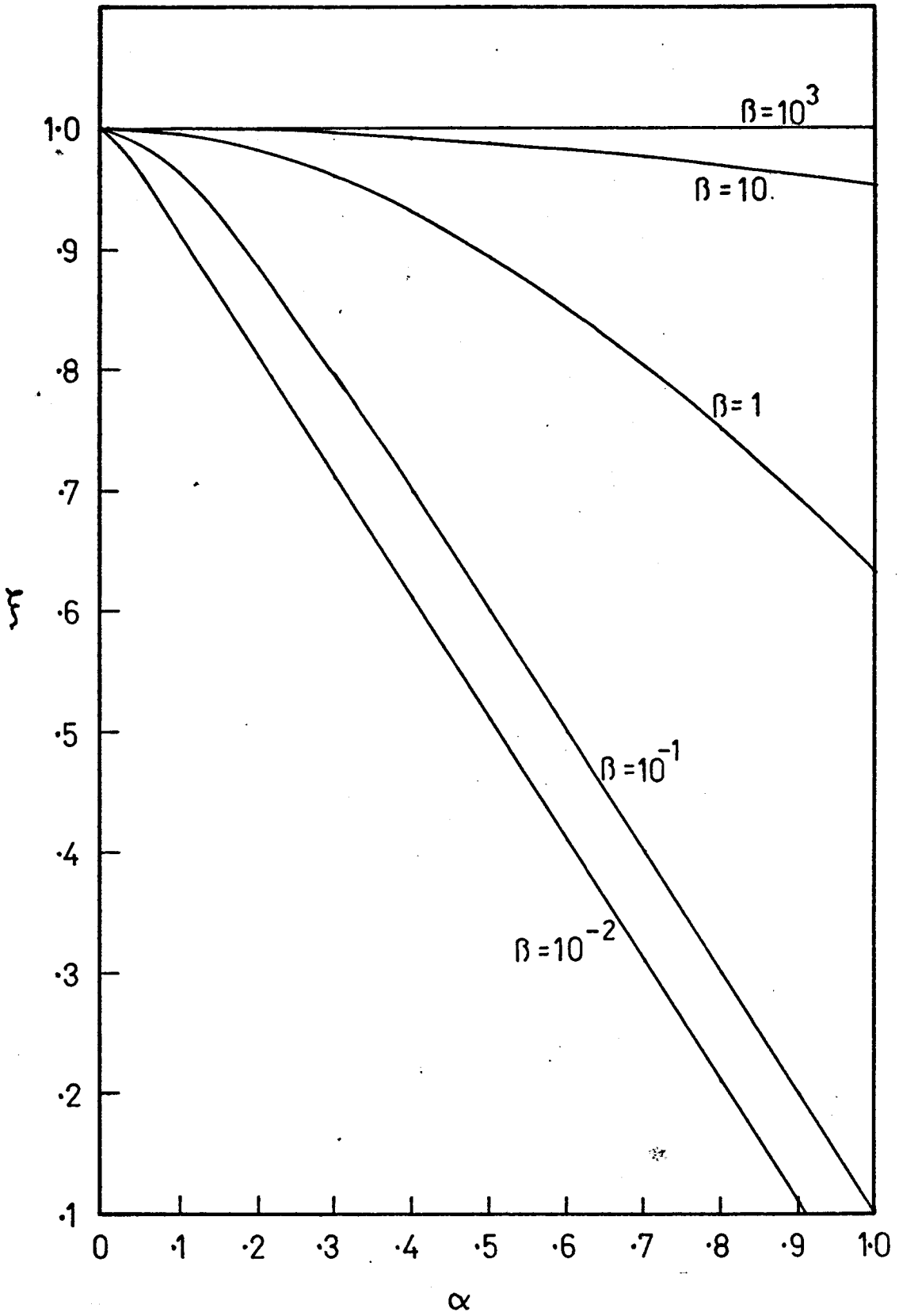

FIG. 3

In order to obtain the response function for a counter with preferential trapping, assume that the probability of the interaction of charged particles across the region from o to d is uniform, that is P(d) is a constant. Then by a change of variable the response function is:

$$P(\xi) = P(\alpha) \left|\frac{d\alpha}{d\xi}\right| = \frac{N}{(1-e^{-\alpha/\beta})} \quad . \tag{12}$$

N is a constant of normalization which will be evaluated for the limits of ξ after all approximations have been made. Experimentally the relative broadening of pulse height spectra peaks due to trapping in damaged counters is small so that it can be assumed that β is large. By expanding the exponential, equation 12 can be approximated by:

$$P(\xi) = \frac{N}{1-1+\frac{\alpha}{\beta}} = N\frac{\beta}{\alpha} \tag{13}$$

By similarly expanding equation (11) and ignoring terms of order in β greater than $(\frac{1}{\beta})^2$ the expression for ξ becomes:

$$\xi = 1 - \alpha + \beta(1 - 1 + \frac{\alpha}{\beta} - \frac{\alpha^2}{\alpha\beta^2} + \ldots) = 1 - \frac{\alpha^2}{2\beta} \tag{14}$$

By combining equations (13) and (14),

$$P(\xi) = \frac{N}{\sqrt{\frac{2}{\beta}(1-\xi)}} \qquad (15)$$

is obtained.

Equation 15 is a closed form approximation of the response function and is subject to the limits of the values of ξ determined by α in equation (11). For $\alpha = 0$, the maximum value of ξ is established as:

$$\xi = 1.$$

For $\alpha = 1$ the minimum value of ξ is found to be:

$$\xi = \beta(1 - e^{-\frac{1}{\beta}})$$

$$\approx 1 - \frac{1}{2\beta} .$$

This was found by expanding the expression as a power series in $\frac{1}{\beta}$ and dropping terms of order higher than $\frac{1}{\beta^2}$. In order to ensure the integrity of the normalization of the response function after all the approximations have been made, N is evaluated by integrating $P(\xi)$ over the interval $[1 - \frac{1}{2\beta}, 1]$ and the result is equated to unity.

$$\int_{1-\frac{1}{2\beta}}^{1} P(\xi)d = \frac{N}{\sqrt{\frac{2}{\beta}}} \int_{1-\frac{1}{2\beta}}^{1} \frac{d\xi}{\sqrt{1-\xi}}$$

$$= -\frac{N}{\sqrt{\frac{2}{\beta}}} \frac{1}{\frac{1}{2}} (1 - \xi) \Big|_{1-\frac{1}{2\beta}}^{1}$$

$$= N$$

$$= 1 .$$

Therefore the response function is given by:

$$P(\xi) = \frac{1}{\sqrt{\frac{2}{\beta}(1-\xi)}} \qquad (16)$$

Figure (4) shows the form of this function for various values of β. It can be seen that by convolving a Gaussian over this function, the resulting form would resemble very closely the shape of a pulse height spectrum peak in which trapping is evident. As the value of β is decreased, tailing on the low energy side of the peak increases. This compounds to an increased loss of charges.

In order to relate this response function and specifically, β, to the observed data it is necessary to formulate some easily measured quantities. For this purpose two that are suitable are the model energy or the most probable peak position and the mean position of the peak. The most probable peak position is located at the point where:

$$\frac{dP(\xi)}{d\xi} = 0$$

That is:

$$\frac{1}{2\sqrt{\frac{2}{\beta}}}(1 - \xi)^{-\frac{3}{2}} = 0$$

In this case:

$$\xi = \lim_{\xi \to 1} \xi$$

$$= 1 . \qquad (17)$$

FIGURE 4

Response function $P(\xi)$ with different β

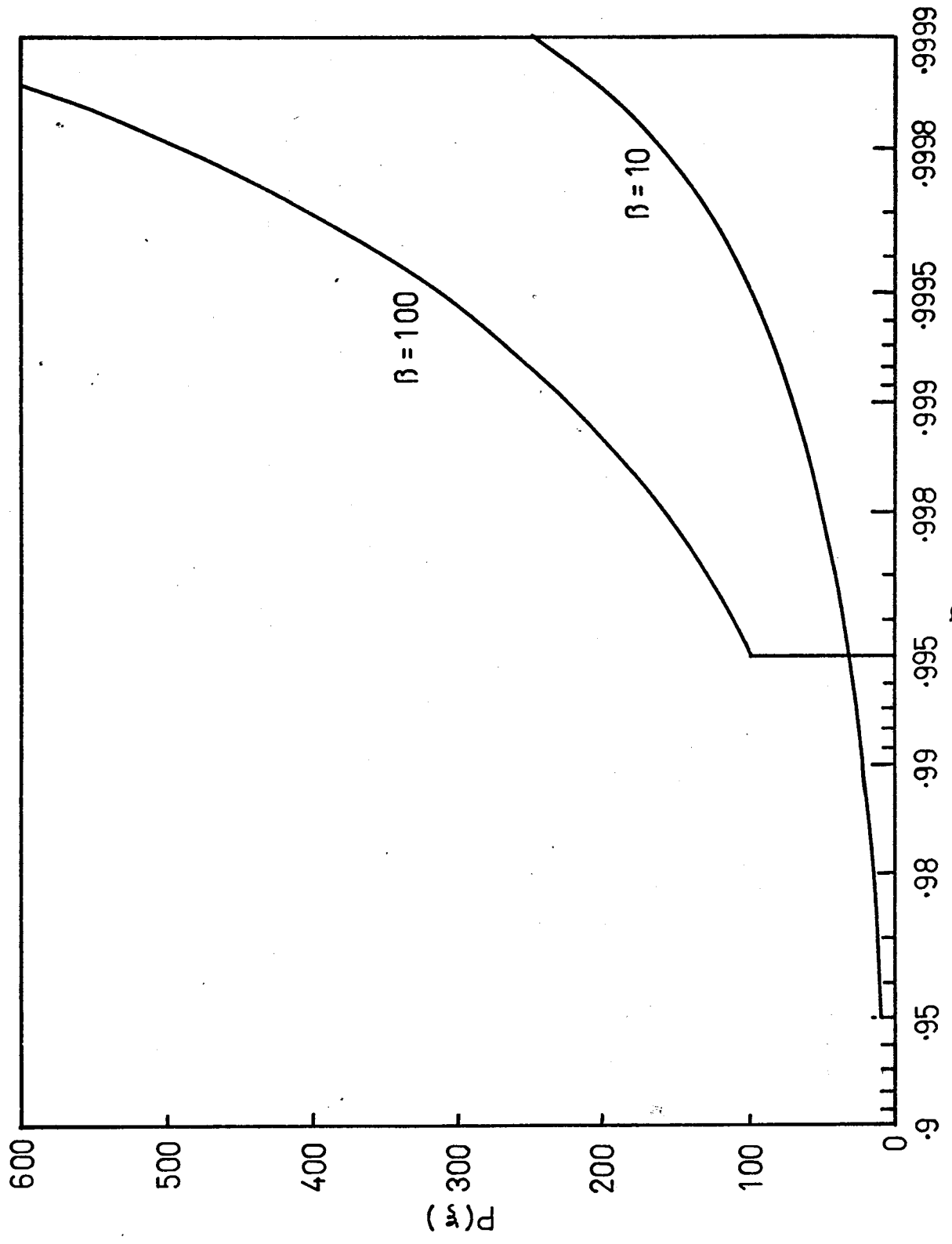
600
500
400
300
200
100
0
P(ξ)
·9
·95
·98
·99
·995
·998
·999
·9995
·9998
·9999
ξ
β=100
β=10

FIG. 4

Another easily measured quantity is the mean of distribution:

$$\bar{\xi} = \int_{1-\frac{1}{2\beta}}^{1} \xi \, P(\xi) d\xi$$

$$= \frac{1}{\sqrt{\frac{2}{\beta}}} \int_{1-\frac{1}{2\beta}}^{1} \frac{\xi}{\sqrt{1-\xi}} \, d\xi$$

$$= - \frac{1}{\sqrt{\frac{2}{\beta}}} \frac{2(2+\xi)}{3} \sqrt{1-\xi} \Bigg|_{1-\frac{1}{2\beta}}^{1}$$

$$= 1 - \frac{1}{6\beta} \quad . \tag{18}$$

Using ξ mode and $\bar{\xi}$ the quantity

$$\Delta = \xi_{mode} - \bar{\xi}$$

$$= \frac{1}{6\beta} \tag{19}$$

is found. This can be calculated easily enough from gamma ray spectra. The mean carrier lifetime can be inferred from equation (19) when it is remembered that $\beta = \frac{\tau}{T_o}$ and that

$$T_o = \frac{d}{v_o}$$

$$= \frac{d}{\mu_E}$$

$$= \frac{d^2}{\mu_v} \tag{20}$$

is the collection time. Here, μ is the mobility of the trapped carrier and v is the applied voltage.

2.6 Width of Pulse Height Peaks

Normally in a counter where trapping is insignificant, the variance of pulse height peak distributions is given by[15]:

$$\sigma^2 = FE\varepsilon + b \qquad (21)$$

where F is the fano factor, $\varepsilon \approx 2.98$ is the average energy required to produce one electron hole pair and b is the contribution by electronic noise in the analysing system. When trapping begins to make a significant contribution to peak width equation (21) is altered by the addition of another term to get:

$$\sigma^2 = FE\varepsilon + b + \sigma_t^2 E^2. \qquad (22)$$

The value of σ_t^2 may be estimated by making the variance of $P(\xi)$.

$$\sigma_t^2 = \int_{1-\frac{1}{2\beta}}^{1} (\xi-\bar{\xi})^2 P(\xi)d\xi$$

$$= \int_{1-\frac{1}{2\beta}}^{1} {}^2P(\xi)d\xi - 2\bar{\xi}\int_{1-\frac{1}{2\beta}}^{1} \xi P(\xi)d\xi + \xi^2$$

$$= \frac{1}{45\beta^2}. \qquad (23)$$

Since β varies inversely as the number of damage or trapping centres and it is reasonable to expect these to vary directly with irradiation time providing the fast neutron

flux is constant, then it can be said that:

$$\beta \alpha \frac{1}{t_{irrad}} .$$

Then the variance of the pulse height distribution would be given by:

$$\sigma^2 = FE\varepsilon + b + \frac{E^2}{.45\beta^2}$$

$$= FE\varepsilon + b + \frac{36}{45} \Delta^2 E^2 \qquad (24)$$

where c is a proportionality constant and t is the irradiation time.

CHAPTER 3

EXPERIMENTAL ARRANGEMENTS

3.1 Introduction

In the verification of the theory developed in the last chapter, it is necessary to have a counter that has been damaged and for which an accurate record of the history of irradiation has been obtained. This would involve subjecting the detector to a beam of fast neutrons of known quantity and periodically measuring its response to gamma radiation.

In the first step the major difficulty lies in the determination of the number of neutrons that interact with the germanium counter. It is known that the average energy of the neutrons obtained from fission is about 1 MeV.

For 1 MeV neutrons a very prominent peak in the response spectrum is the 691 keV line which arises from the production of conversion electrons from ^{72}Ge. The detection of these electrons and the subsequent x-rays proceeds with almost 100% efficiency. Chasman et al[1] found that the cross-section for the production of this reaction in natural germanium was about 80 mb. Thus by monitoring the number of 691 keV events occurring during irradiation the neutron flux was calculated.

In order to monitor the detector response to gamma ray radiation, two alternatives are available. One is to place a gamma ray source in the neutron beam along side the counter so that gamma rays produced by the neutron-induced reactions of the same can be detected by the device. Another means is to interrupt irradiation of the counter periodically and measure gamma rays from a source. In the actual experiment performed, both means were used. While the latter method gave adequate results the former was not quite as successful because the high intensity of gamma rays from the reactor core provided a count rate that was too high for reliable results. The limited time available for irradiation precluded the possibility of attenuating the gamma rays which would have decreased the neutron flux as well.

3.2 Irradiation of Planar Detectors

Two planar Ge(Li) counters were irradiated with fast neutrons. The first detector was fabricated from germanium supplied by Hoboken using techniques described in another paper[3] . It had an active volume of about 0.4 cc. and the width of the intrinsic region was about 0.4 cm. During irradiation it was operated with an electric field of 400 volts/mm. The second detector was supplied by Sylvania Electronic Products Co. It had an active volume of about 1.6 cc. and the width of the intrinsic region was about 0.4

cm. Its applied electric field during irradiation was 180 V/mm.

Both counters were mounted in a special long vacuum chamber that was designed for irradiations in the beam port facility. This chamber is illustrated in Figure (5). It consisted of a four foot long narrow evacuated enclosure made from aluminum pipe. On the upper end a VACION pump was attached to maintain the vacuum. Extending down the length of the pipe was the hollow "cold finger", which had a detector holder attached to the end of it. The detector end was enclosed by an aluminum cap on a rubber O-ring. A liquid nitrogen cryostat was mounted on top to drip feed liquid nitrogen into the cold finger. The long chamber was installed in the fast neutron beam port facility by inserting it through a hole, in a platform laid across the shielding tanks, to a level determined by the movable collar. The level of the collar was adjusted so that when the chamber was in position the detector in its holder was at the same level as the neutron beam.

Once mounted, both planar detectors were checked for preferential carrier trapping. This was carried out after the example of P. P. Webb et al[6], by using a collimated source mounted on an adjustable platform. This could be raised and lowered, thus allowing the source to be aimed at different positions in the counter. This ap-

FIGURE 5

Vacuum chamber for irradiating detectors

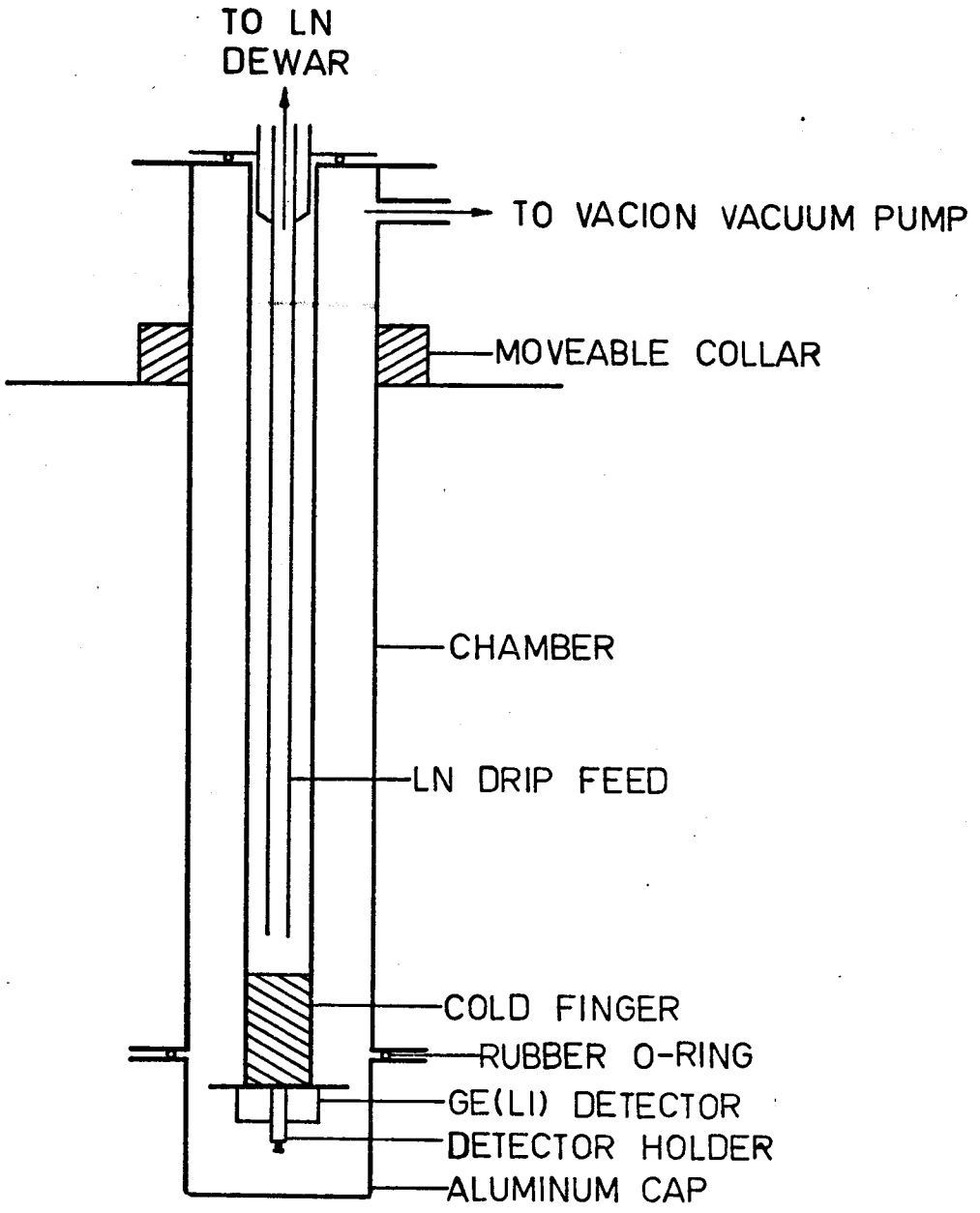

FIG. 5: VACUUM CHAMBER

paratus is shown in Figure (6). Pulse height spectra of the response of the detector to gamma rays aimed at 1.0 mm. intervals across the width of the counter were then measured using a Canberra 1408B preamplifier, a Canberra amplifier and a Nuclear Data ND 150 M 1024 channel pulse height analyzer.

In this way the different distances having to be traversed by each charged carrier would cause different amounts of trapping at different collimated source positions. This would show up as varying amounts of skewness in the pulse height peak for the gamma ray.

The source was made by drilling holes into either side of a 2 inch wide lead brick so that they met. One hole was $\frac{3}{16}$ inches in diameter and $\frac{3}{4}$ inches deep and served to contain the gamma ray sample. The collimating hole was $\frac{1}{32}$ inches in diameter and 1-1/4 inches deep. For the source of gamma radiation a sample of ^{203}Hg giving off 10 mc of gamma rays with an energy of 279 keV was used.

The advantages that led to the choice of this sample were that the long half life of 47 days enabled the collimated source measurement to be carried out over a period of several days without significant loss of intensity. Also, with higher energies, the amount of dispersion of radiation in the germanium increases significantly so that the resolution of the measurement is impaired. This point was especially important since diameter of the chamber and the small size

FIGURE 6

Collimated gamma-ray source

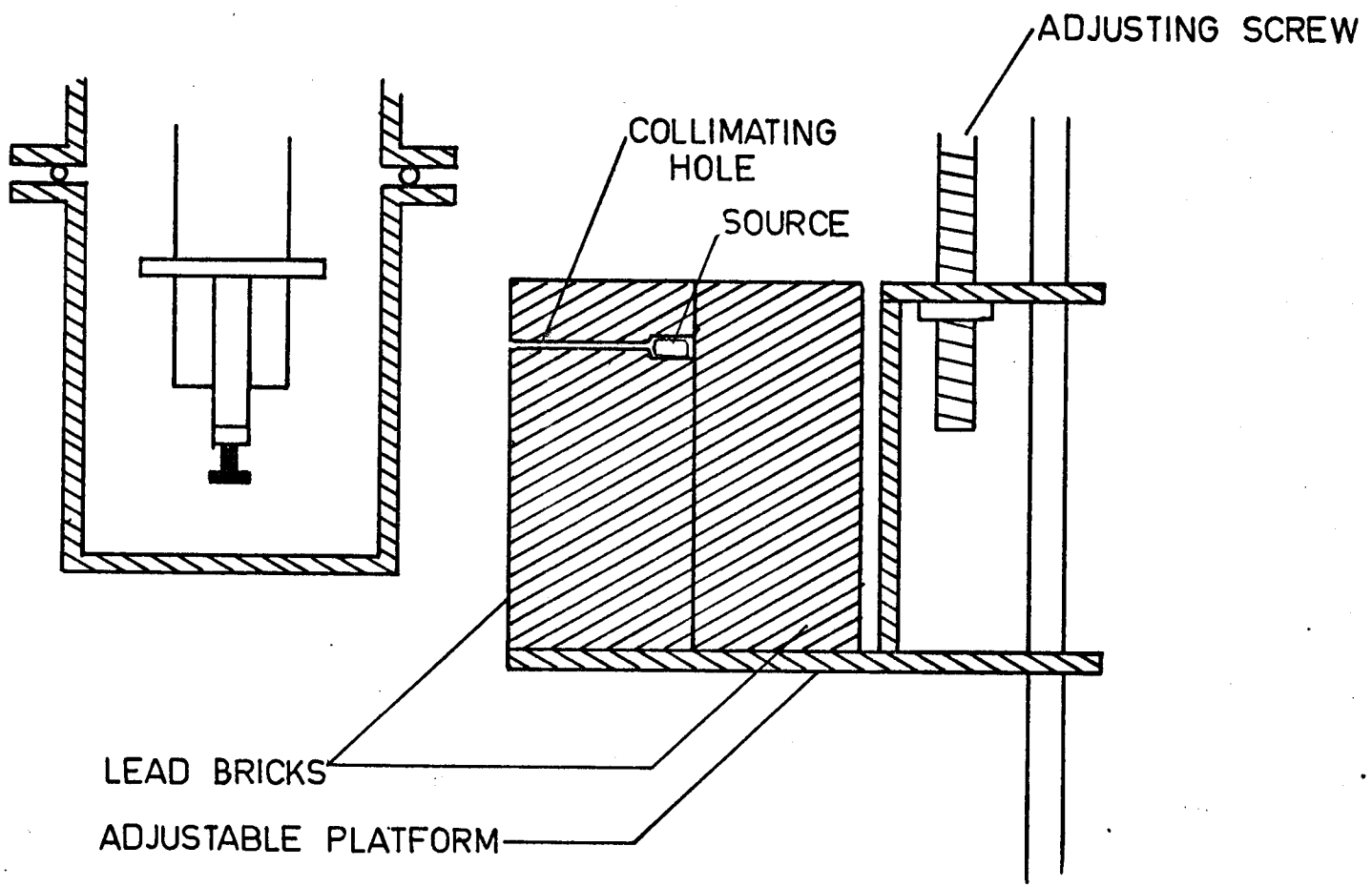

FIG. 6: COLLIMATED GAMMA RAY SOURCE

of the counter resulted in the collimator to counter distance being a large fraction of the source to counter distance.

In the arrangement of the chamber during irradiation in the fast neutron beam port facility a reinforced wooden platform was set across the tops of the water-shielding tanks. An oval shaped hole in the platform enabled the counter chamber to be moved laterally in and out of the neutron beam. Vertical adjustment was allowed by the movable clamped ring on the shaft of the chamger. A heavy lead shutter controlled by a switch outside the water tanks opened and closed the neutron beam port, thus allowing one safe access to the top of the water tanks to adjust the counter position.

The electronic system used to monitor the counter response and the intensity of the 691 keV peak arising from inelastic scattering included the Canberra preamplifier and amplifier mentioned earlier and a Nuclear Data ND 3300 4096 channel pulse height analyzer.

For the 0.4 cc counter, the data were analyzed continuously and dumped onto magnetic tape at intervals of 20, 40 and 80 minutes. For the 1.6 cc detector the data were analyzed for two 15 minute periods every day. For both counters, the position of the chamber in the beam was changed several times and for each change, the 691 keV line was monitored to determine the intensity of neutrons irradiating it.

For both counters, irradiation was interrupted at intervals in order to measure their response to gamma rays of energies up to 2.6 MeV. from a thorium source. For each counter irradiation proceeded for a period of about 5 days. Again for each, this exposure time was necessarily limited by a shutdown of the nuclear reactor.

After irradiation each detector was then checked for preferential carrier trapping using the collimated source technique.

The third detector was a much larger unit, about 15 cc., compared with the others and was of the single open-end coaxial configuration rather than planar. The history of damage of this counter was also very different. This counter was originally involved in a different experiment with collimated x-rays ranging in energies from 1.8 MeV. to 10.8 MeV originating from a source beside the reactor core. This beam port is described in another source[7]. The relatively high mass of the sample also scattered fast neutrons down the collimator with the result that the gamma ray beam was contaminated by high energy neutrons. It was not possible to shield the counter from the neutrons without significantly attenuating the gamma radiation. Thus a very accurate record of the deterioration of this detector due to damage from fast neutron irradiation was obtained over a period of about 1-1/2 months. The total in-

tegrated neutron flux received by the counter in this time was about 0.6×10^{10} neutrons.

In this experiment gamma rays were analyzed after passing through an absorber for twenty minutes and then without being absorbed for five minutes in alternating periods. This was done with a pair spectrometer and amplifier system gated in such a way that only double escape events were analyzed by the Nuclear Data ND 3300 analyzer. The output was also stabilized with respect to gain shift and zero shift on peaks from a double peak precision pulser. After each period of analyzing with and without the absorber, the spectrum was dumped onto magnetic tape and then summed in a computer. Since the system was responding only to double escape events, the actual energies analyzed by the detector ranged from 0.757 MeV to 9.805 MeV. In all, 9 composite spectra were obtained, each representing a different period in the history of the counter and each showing a chancing response to gamma rays due to irradiation damage.

CHAPTER 4

IRRADIATION EFFECTS

4.1 Planar Detector "A"

The first part of the investigation of this counter involved scanning the device from the p-region, across the intrinsic to the n-region with a columated gamma source. Figure (7) shows the amount of skewness in the detector response spectrum to the gamma source as the collimator was scanned across the detector in increments of 1.0 mm. Note that the abscissa represents only the incremental changes in collimator position and not any particular distance relative to the counter dimensions. The figure shows the ratio of peak height to peak area for each of the increments. It can be seen that because of the low energy of the gamma source used in the collimator the change in response is slight but is, nevertheless, large enough to show evidence of some preferential charge trapping. This figure does show that skewness was more pronounced when the collimator was aimed close to the p region. As well, Figure (7) shows that as the collimator was moved toward the n-region, the ratio of peak height to the peak area increased slightly, indicating that a greater percentage of the detector signals were included closer to the mode position. From these it

FIGURE 7

Ratio of peak height to peak area against position of collimated source for detector A before irradiation.

Skewness against position of collimated source for detector A before irradiation.

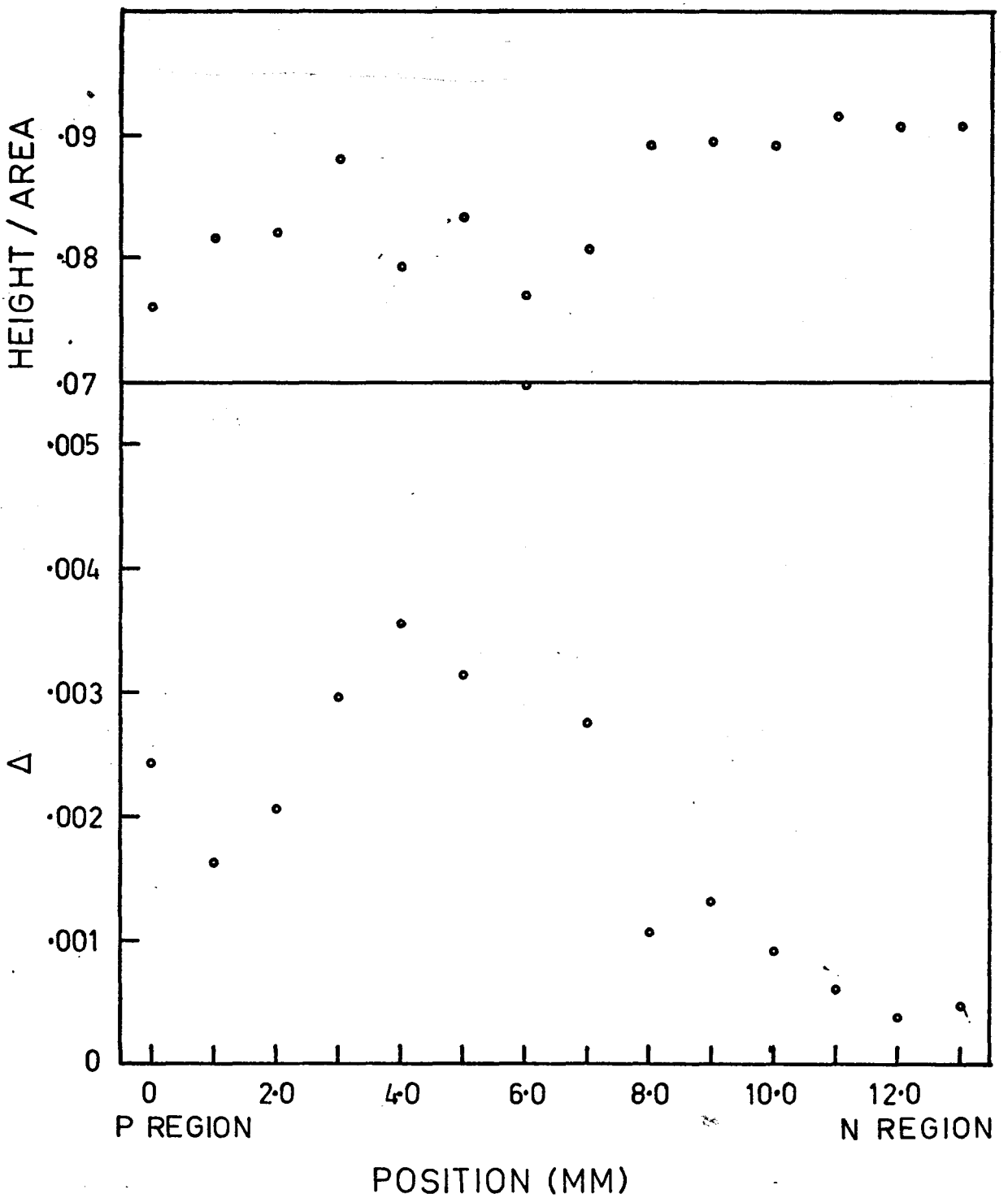
HEIGHT / AREA
·09
·08
·07
·005
·004
·003
·002
·001
0
Δ
0
2·0
4·0
6·0
8·0
10·0
12·0
P REGION
N REGION
POSITION (MM)

FIG. 7

can be seen that the carriers that were trapped more were those that had to traverse the full width of the intrinsic region, that is, the electrons.

When the counter was irradiated with high energy neutrons, skewness in the pulse height spectrum for thorium C" quickly became evident as shown in Figure (8). This shows the response to the 2614 keV line collected during interruptions in the irradiation. The integrated neutron flux, I, that the counter was exposed to up to each of these times is shown on the abscissa. It can be seen that by the time the device had been exposed to 2.3×10^9 neutrons over its active volume, the amount of skewness present was enough to render it valueless for normal research.

Table (I) shows the values of Δ found from the thorium C" spectrum taken during each of the interruptions. The accuracy of these values was limited by several considerations. First energy peaks produced from the irradiation process were not suitable for analysis because the high count rate contribution of the gamma flux from the reactor core resulted in distortion from pulse pile up, random summing and high background. Therefore the spectra measured during irradiation could not be used and measurements of Δ were taken from the spectra of gamma rays from the thorium C source, which was limited to energies below 2614 keV. The second consideration was in the limitations brought about by compressing an energy

FIGURE 8

Pulse height peak response of counter to 2614 keV gamma rays for 0 neutrons, 3.2×10^{8} neutrons, 14.4×10^{8} neutrons and 21.8×10^{8} neutrons

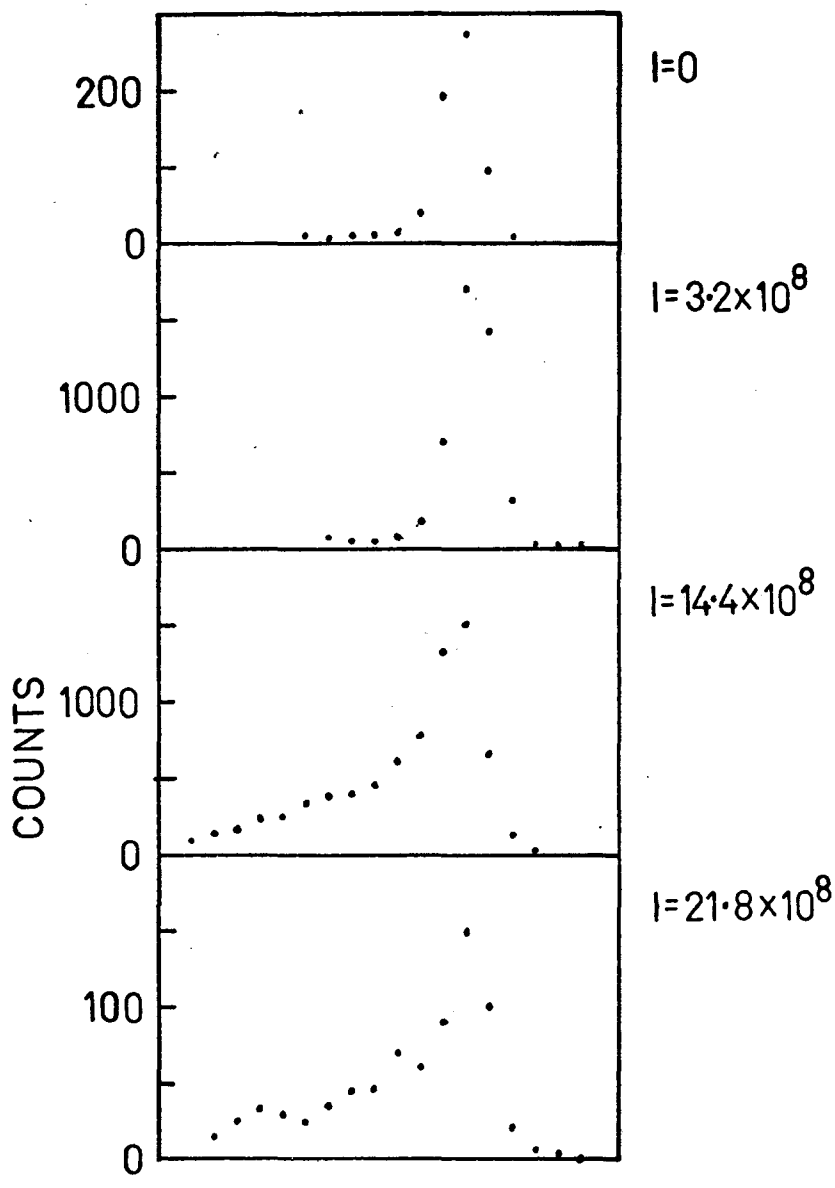

FIG. 8

TABLE I

Skewness at different energies during irradiation

I neutrons / E (keV)	0	3.2×10^8	14.4×10^8	21.8×10^8
2614	0.00008	0.00018	0.00172	0.00300
1592	0	0.00031	0.00341	0.00385
966	0.00071	0.00108	0.00180	0.00341
908	0.00028	0.00073	0.00232	0.00347

range of 2.6 MeV into a scale of less than 1024 discrete channels. The result of this was that each peak consists of about 5 points which can normally be fitted to Gaussian distribution. When skewing is present on the low side of each peak, and one wishes to find the modal position, this course of action becomes more improbable. Such skewing leaves about 3 points on which to fit the Gaussian. Therefore, to arrive at an approximation of the modal position, the mode of a quadratic function that passed through the logarithm of the three points around the top of each peak was calculated. That this estimation is not valid is illustrated by the large relative errors in the values of Δ for the less skewed peaks. The limitations of these values are especially illustrated in Figure (9) which shows Δ plotted against energy. It was assumed on the basis of Chapter II that every Δ value, calculated from a single spectrum, would be independent of energy. However, Figure (9) shows large variations, but encouragement may be drawn from the fact that these tend to cluster somewhat about a certain value of Δ. The average of these Δ for each spectrum is tabulated in Table II.

On plotting the contents of Table II on a graph as shown in Figure (10) it is found that there is a closely linear relationship between $\bar{\Delta}$ and the integrated flux to

FIGURE 9

Skewness, Δ, for different energies at 0 neutrons, 3.2×10^{8} neutrons, 14.4×10^{8} neutrons and 21.8×10^{8} neutrons.

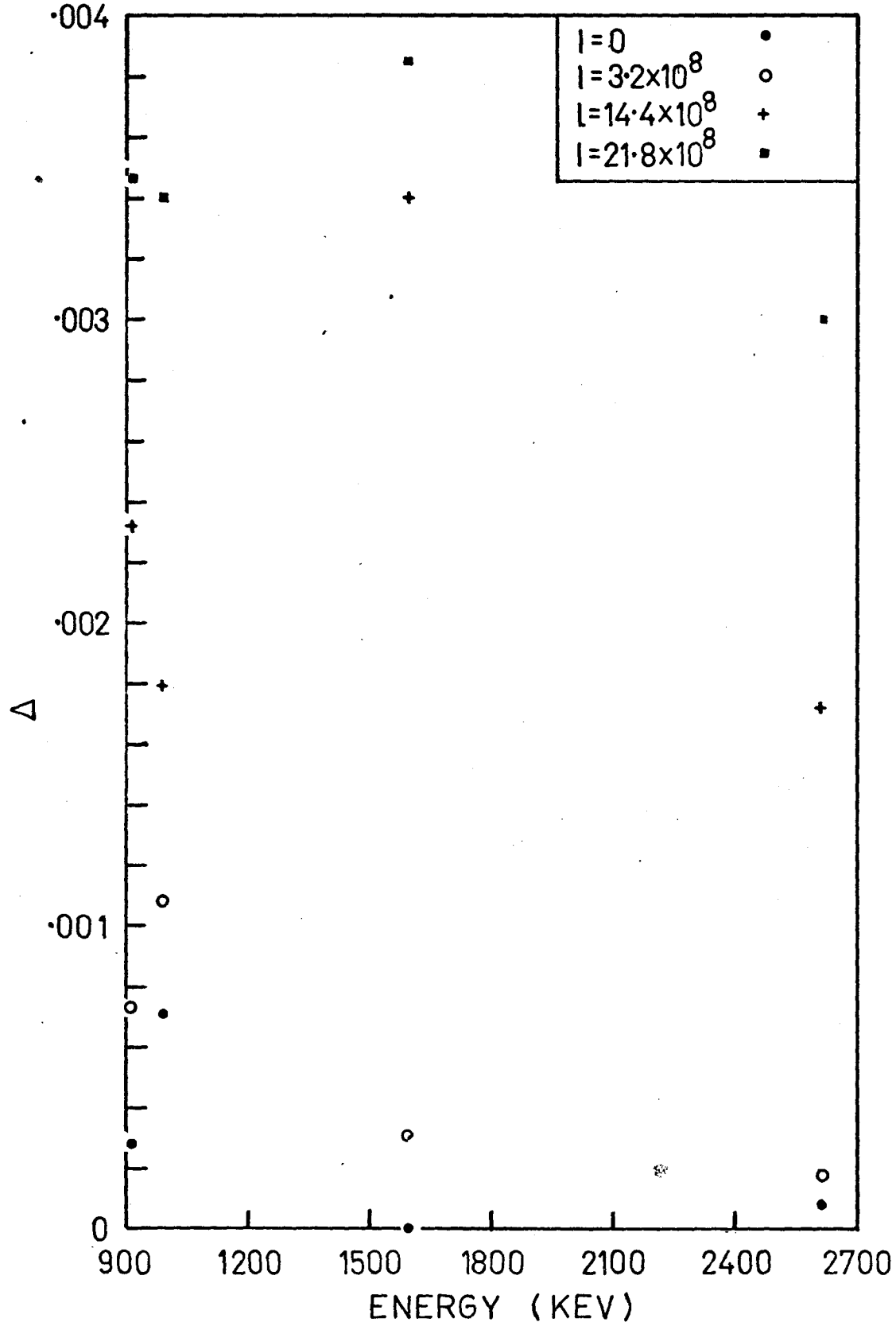
·004
·003
·002
·001
0
Δ
I = 0
I = 3·2x10^8
I = 14·4x10^8
I = 21·8x10^8
900
1200
1500
1800
2100
2400
2700
ENERGY (KEV)

FIG. 9

TABLE II

Average skewness during irradiation

Accumulated incident neutrons	$\bar{\Delta}$
0	0.00012 ± 0.00023
3.2×10^8	0.00058 ± 0.00041
14.4×10^8	0.00231 ± 0.00078
21.8×10^8	0.00343 ± 0.00035

FIGURE 10

Average skewness measured during irradiation

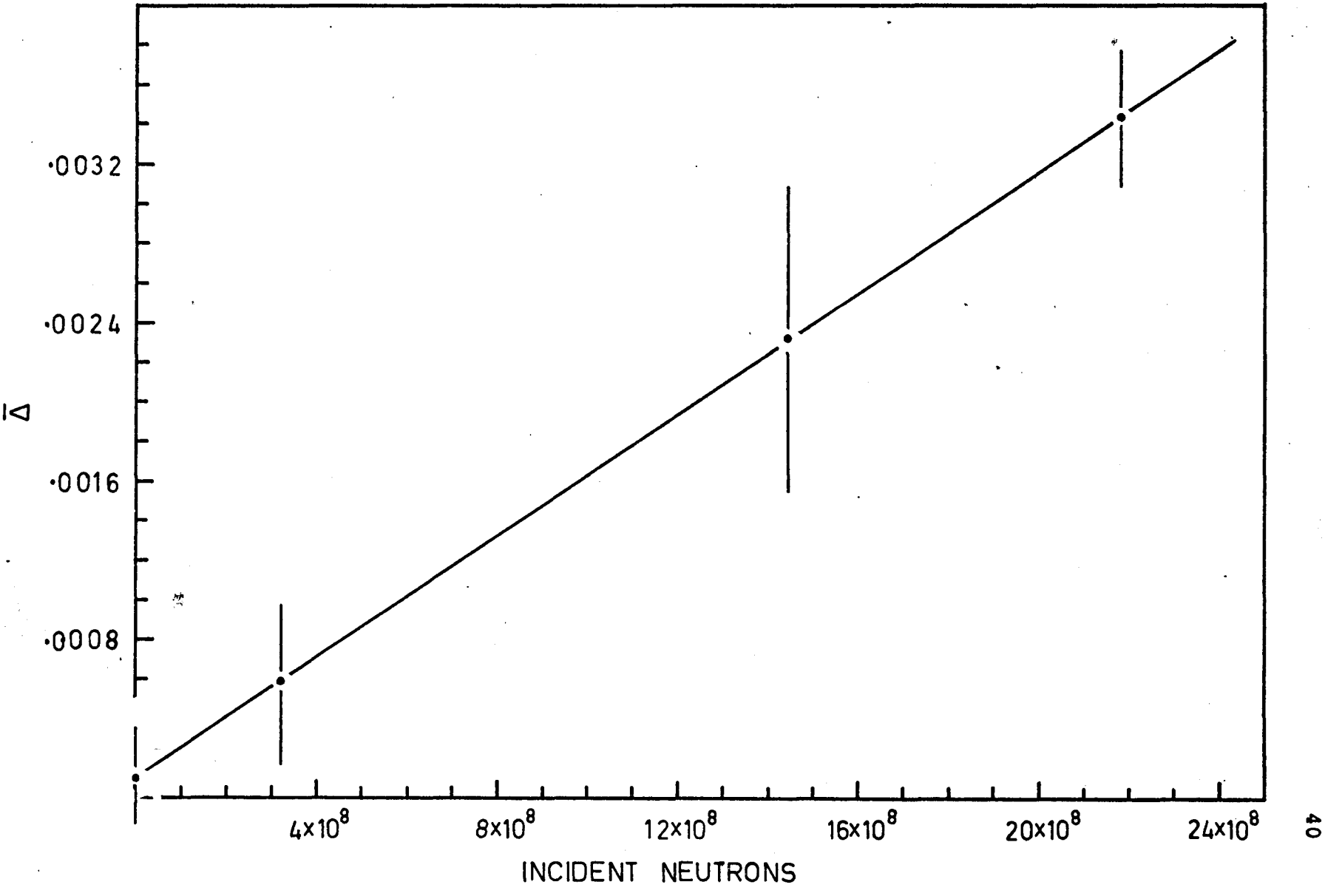
·0032
·0024
·0016
·0008
|Δ|
4x10^8
8x10^8
12x10^8
16x10^8
20x10^8
24x10^8
INCIDENT NEUTRONS

FIG. 10

which the counter had been exposed. This observation is a reasonable one to make since the life time of the carrier would be inversely proportional to the number of trapping centres which is again proportional to the number of damaging neutrons that have been stopped by the counter. A linear least squares fit reveals that the equation of this relationship is:

$$\Delta = 1.5 \times 10^{-12} \, I + 1.1 \times 10^{-4} \qquad (25)$$

By substituting equation (25) into equation (24) an expression is obtained for the variance of a pulse height peak.

$$\sigma^2 = F_\varepsilon E + \sigma^2_{elect} + \frac{36}{45} (1.5 \times 10^{-12} \, I + 1.1 \times 10^{-4})^2 \, E^2 \qquad (26)$$

For the electronic system used in this investigation one value of σ_{elect} was 1.53 keV. Before irradiation, the intrinsic contribution of the counter to the FWHM at about 1 MeV was about 2.0 keV. For an energy per charge pair of 3.0 eV, this gives a value of 0.51 for the fano factor, F. Thus the FWHM for this counter as a function of energy and neutron dose is:

$$\text{FWHM} = 2.35 \, \sigma$$

$$= 2.35 (1.53 \times 10^{-3} E + 2.34 + 0.8 (1.5 \times 10^{-12} I + 1.1 \times 10^{-4})^2 E^2)^{\frac{1}{2}}$$

for E measured in keV. This is shown as a function of neutron dose for various values of energy in Figure (11).

FIGURE 11

Variation of FWHM of detector A and analyzing system during irradiation for various energies.

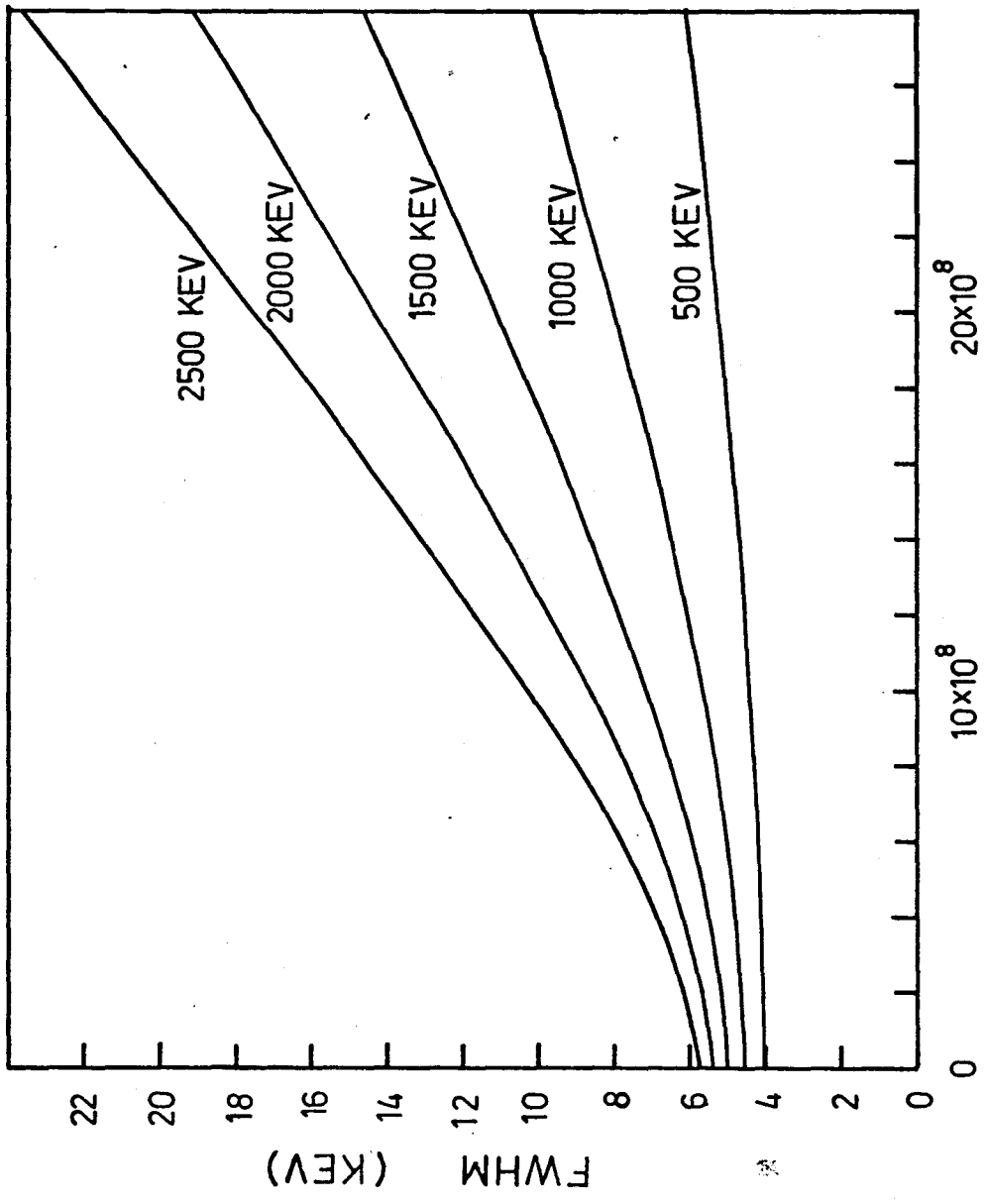
2500 KEV
2000 KEV
1500 KEV
1000 KEV
500 KEV
FWHM (KEV)
22
20
18
16
14
12
10
8
6
4
2
0
0
10x10^8
20x10^8
INCIDENT NEUTRONS

FIG. 11

After irradiation had taken place, another investigation of the preferential trapping occurring was made with the columated source. This is shown in Figure (12). This time the ratio of the peak height to peak area is more indicative of electron trapping. The amount of skewness in the peak shows a smooth decrease toward the n-region while the spurious beginning is difficult to interpret without considering scattering effects from the detector mount.

The number of defects producing the trapping in the count can be calculated from a knowledge of the number of neutrons. Kraner et al[2] calculated that the average energy deposited in atomic collisions for each neutron at an energy of 1.1 MeV was 2.6 keV/cm^3. By assuming that the fission neutron spectrum has an average energy of 1 MeV, and that 20 eV is required to produce a defect in a germanium lattice, then one would calculate that each neutron produces about 130 defects per cc. For the counter just described, the number of defects produced by irradiation would then be about 1.4×10^{11} in its active volume.

4.2 Planar Detector B

The result of the collimated source experiment before irradiation is summarized in Figure (13) It is again seen that the values obtained for Δ tended to decrease as the collimated source was swept away from the p region. This

FIGURE 12

Ratio of peak height to peak area agsinst collimated source position for detector A after irradiation.

Skewness against collimated source position for detector A after irradiation.

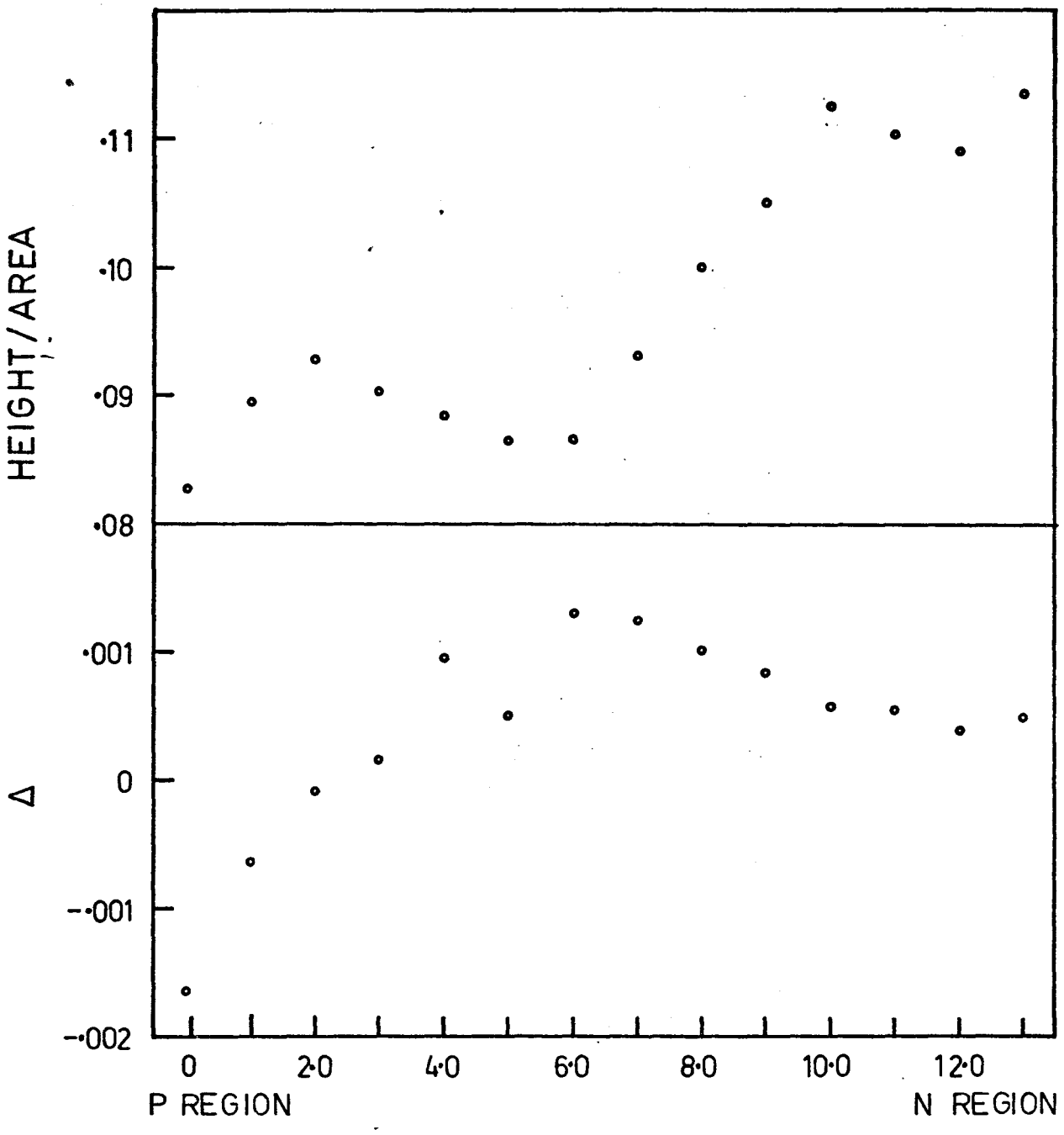
HEIGHT/AREA
·11
·10
·09
·08
Δ
·001
0
-·001
-·002
0
2·0
4·0
6·0
8·0
10·0
12·0
P REGION
N REGION
POSITION (MM)

FIG. 12

FIGURE 13

Ratio of peak height to peak area against collimated source position for counter B before irradiation.

Skewness against collimated source position for counter B before irradiation.

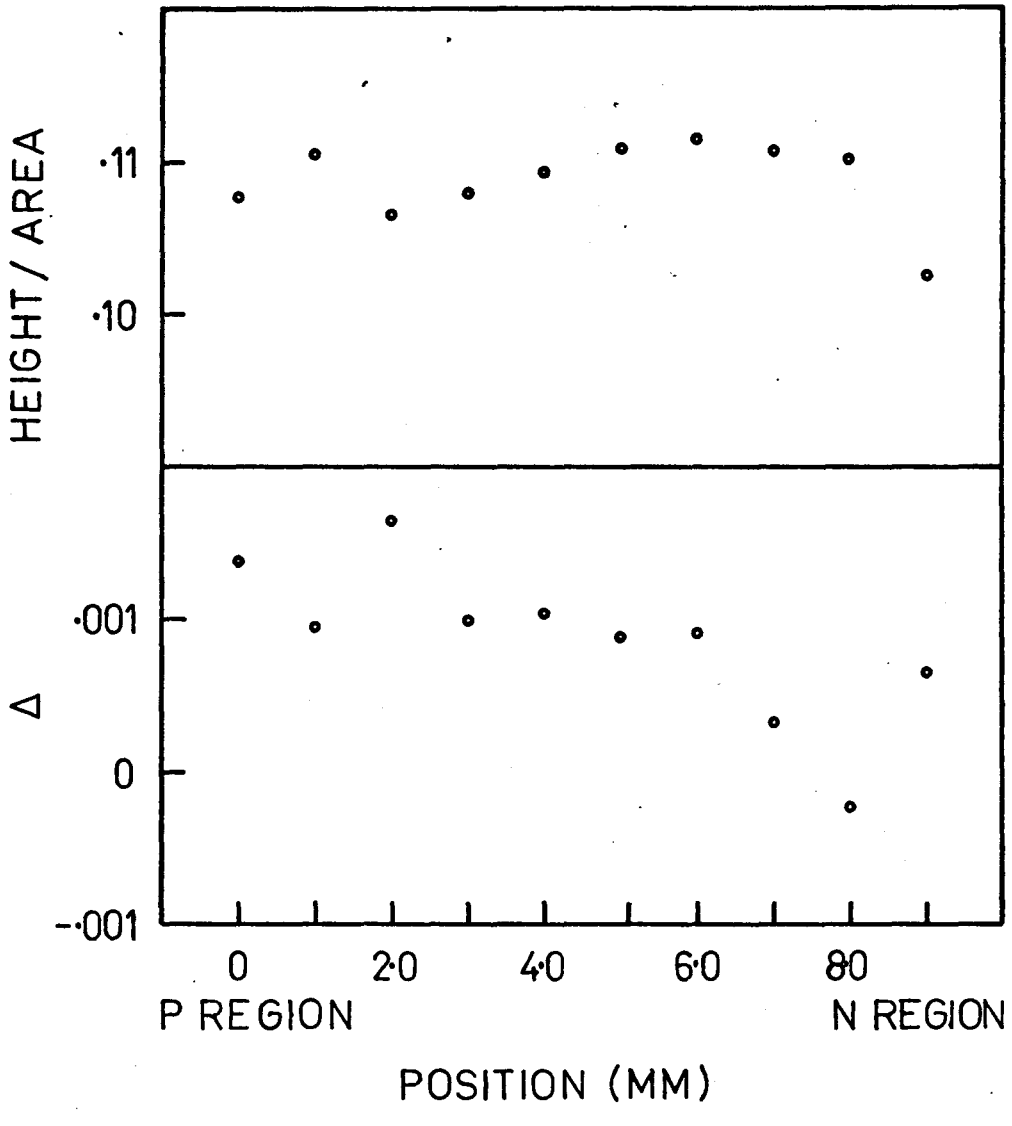
HEIGHT / AREA
·11
·10
Δ
·001
0
-·001
0
2·0
4·0
6·0
8·0
P REGION
N REGION
POSITION (MM)

FIG. 13

indicates that more electrons than holes were trapped. This conclusion is further supported by the trend of the ratio of the pulse height to the pulse area as shown in the figure. The increase in this ratio as the source was moved toward the n region clearly indicates that the efficiency of the charge collection was also rising. Thus before damage occurred there was preferential electron trapping present in the 1.6 cc planar detector, but as it was stated in the previous section, no conclusion can be drawn on the amount of trapping that occurred.

Due to the limited time available for irradiation of this counter its exposure to neutrons was not interrupted to record its response to gamma rays from the thorium C" source. Instead its response was measured during irradiation and unfortunately these measurements were not reliable for reasons pointed out earlier. It was possible, however, to make some determination of the change of Δ with neutron dose by assuming a linear relationship and by fitting it to the average $\bar{\Delta}$ found before and after irradiation. Those Δ that were found before are given in Table III and the corresponding average was 0.00018 ± 0.00008. The Δ measured after irradiation are given in Table IV. Their average value was 0.00081 ± 0.00030. Over a period of 47 hours a total of 6.8×10^8 neutrons, as calculated from the 691 keV line during irradiation, were incident upon the detector. From this, the relation

TABLE III

Skewness measured before irradiation

E (keV)	2614	1592	966	908
Δ	.000137	.000115	.000291	.000192

TABLE IV

Skewness measured after irridiation

E (keV)	2614	1592	966	908
1	.000701	.000763	.001481	.000570
2	.000655	.000787	.000938	.000459
3	.000709	.000713	.001305	.000649

$$\Delta = 0.92 \times 10^{-12} I + 1.84 \times 10^{-4} \qquad (28)$$

describing the change of Δ with accumulated neutrons, is obtained.

An expression for the FWHM of the pulse height peak for this counter is found to be, using Equations (24) and (28),

$$FWHM=2.35(1.5\times10^{-3}E + 2.25+0.8(.92\times10^{-12}I + 1.84\times10^{-4})^2E^2)^{\frac{1}{2}}$$

Here a Fano factor of 0.5 and σ_{elect} of 1.5 keV was used in arriving at this result. Figure (14) shows the variation of the FWHM given in Equation (29) for various energies over the lifetime of this counter.

After neutron exposure, the collimated source was again used to explore for signs of preferential trapping. The results, shown in Figure (15) are indicative of a preference for the trapping of electrons, but not as conclusively as for that before irradiation. The values of Δ had no major tendency to change during the scan of the collimated source across the intrinsic region. The ratio of the peak height to the peak area did however increase as the source was moved toward the n region, thus showing that greater charge collection efficiency occurred nearer to the region. This could indicate that there was a preference for electron trapping. It should be emphasized that, due to the limitations arising from the use of a low energy

FIGURE 14

Variation of FWHM of detector band analyzing system during irradiation for different gamma ray energies.

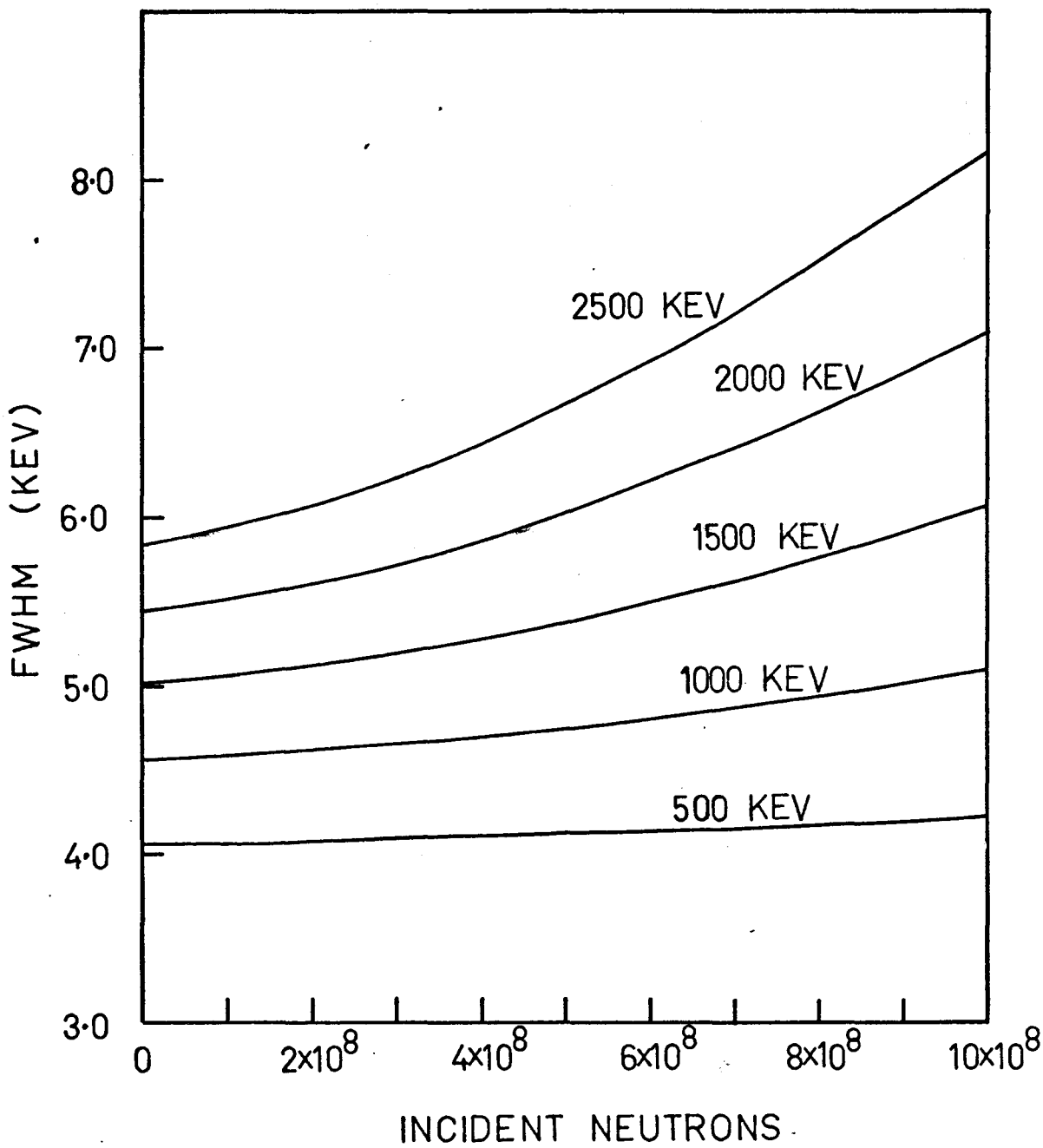
8·0
7·0
6·0
5·0
4·0
3·0
FWHM (KEV)
2500 KEV
2000 KEV
1500 KEV
1000 KEV
500 KEV
0
2x10^8
4x10^8
6x10^8
8x10^8
10x10^8
INCIDENT NEUTRONS

FIG. 14

FIGURE 15

Ratio of peak height to peak area against collimated source position for counter B after irradiation.

Skewness against collimated source position for counter B after irradiation.

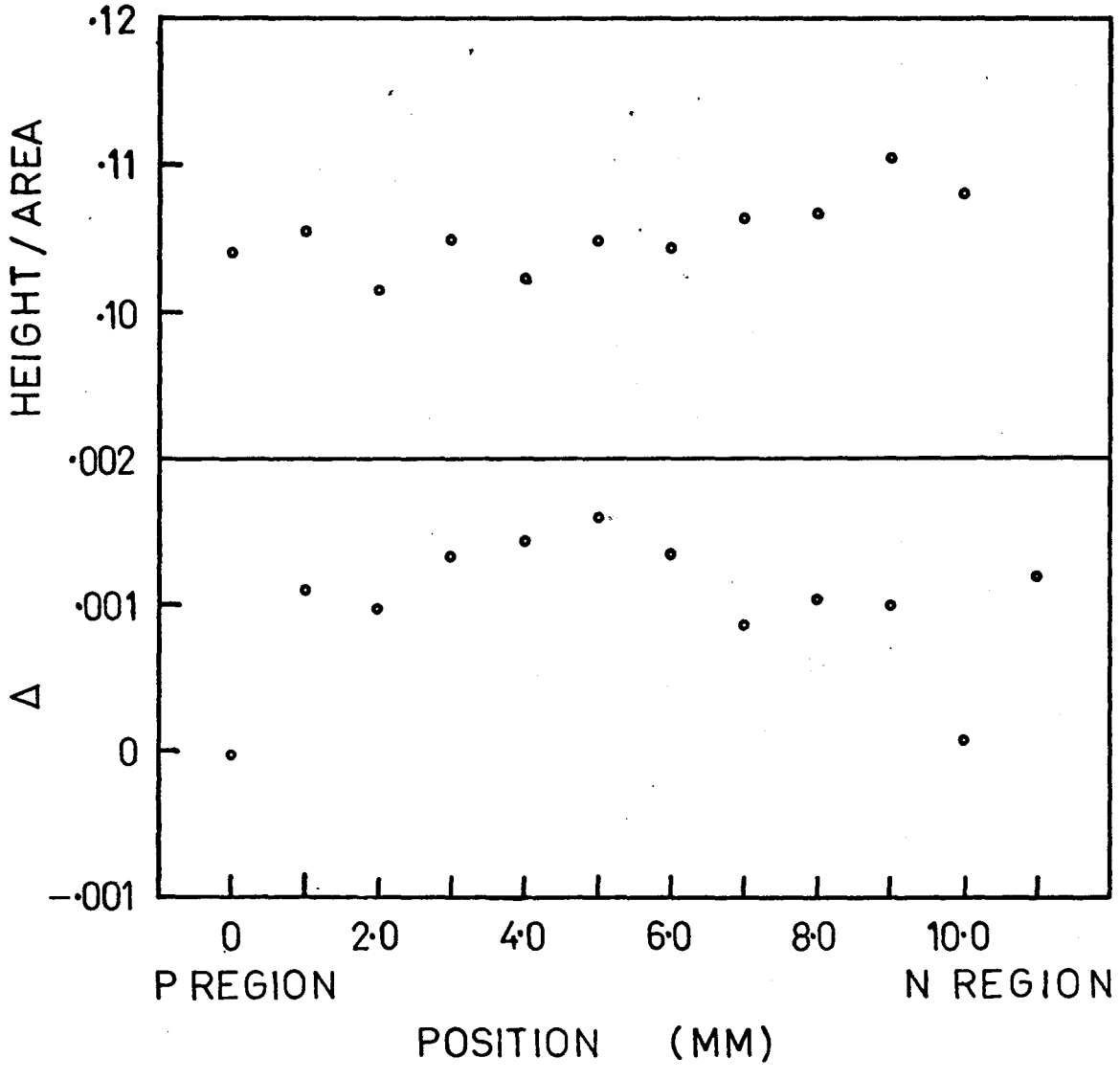

FIG. 15

source, the magnitude of the response of this experiment was not necessarily indicative of the amount of trapping present.

Using the same assumption made at the end of section 4.1 the number of defects corresponding to irradiation by 6.8×10^{8} neutrons would be 0.55×10^{11} defects per cc.

4.3 Single Open-Ended Coaxial Detector

After having seen that neutron irradiation had increasingly greater effects on the response of counter to gamma rays for higher energies, it was thought that a more accurate fit could be made to the preferential trapping model with measurements obtained for gamma ray energies beyond 2.6 MeV.

This opportunity presented itself during the course of another experiment when it was found that high energy gamma ray peaks were beginning to display evidence of fast neutron damage. The counter was being irradiated by neutrons from the nuclear reactor, that were being scattered into the collimator of a source irradiation facility[7].

Subsequent measurements with a neutron monitor showed that the neutron flux was 0.5×10^{10} neutrons per month. Therefore over the duration of this experiment, the counter received a total of 0.6×10^{10} neutrons. An accurate history of the damage was made possible by the complete records maintained during this experiment.

In all, 9 spectra were available, each representing a different period in the life of the instrument. In each of these spectra, the amount of skewness was measured for 11 different energies ranging from 1730 keV to 9805 keV. The corresponding values of Δ are tabulated in Table (V). The confidence with which this data was handled was increased considerably by the large size of the peaks, both in width and in height. The modal positions were, for example, found in a more meaningful fashion by fitting a quartic function to the top 7 points on the peak and solving its derivative for the maximum position. In order to check the consistency of these values, $\bar{\Delta}$ was found for each spectrum and then this was divided into each Δ in the same spectrum, as shown in Table (VI). The result was a series of numbers which, if Δ was relatively constant, clustered around 1.0. Moreover if there is a correlation from spectrum to spectrum, the average quotient for each single energy across all spectra should likewise be clustered very closely about 1.0 as shown in Figure 16. This shows that Δ is indeed without any overt upward or downward trend. Thus the analysis of the data proceeded with more confidence.

In Table (V), row 12, the $\bar{\Delta}$ is given against time. The same plotted on a graph, Figure (17), shows an upward trend that is approximately linear with increasing irradiation

FIGURE 16

Correlation of normalized skewness measured during irradiation against gamma ray energy

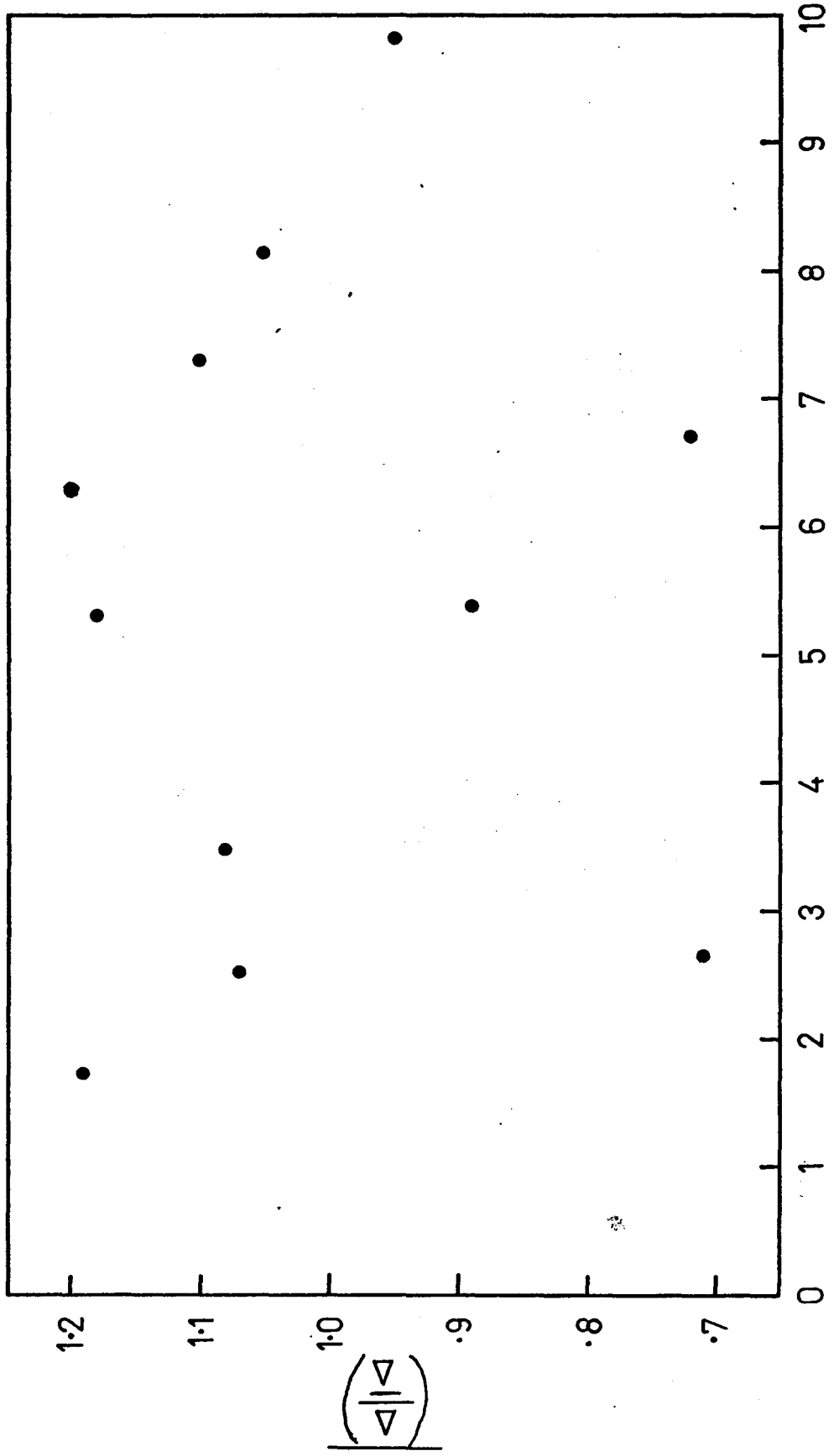
1·2
1·1
1·0
·9
·8
·7
$\left(\frac{\nabla}{\nabla}\right)$
0
1
2
3
4
5
6
7
8
9
10
ENERGY (MEV)

FIG. 16

TABLE V

Skewness at different energies during irradiation

Accumulated Irradiation Time (HR) / Energy (keV)	66	183	270	347	444	550	649	737	812
1732	0.000325	0.000889		0.000557	0.000521		0.001177	0.001075	0.000681
2508	0.000546	0.000570	0.000371	0.000421		0.000640	0.000936	0.001204	0.000644
2653	0.000139	0.000315	0.000160	0.000437	0.000505	0.000465	0.000620	0.000806	0.000661
3486	0.000525	0.000384	0.000434	0.000405	0.000370	0.000703	0.000811	0.001246	0.001393
5299	0.000502	0.000446	0.000413	0.000583		0.000639	0.001003	0.001261	0.001445
5373	0.000200	0.000196	0.000402	0.000509	0.000421	0.000771	0.000760	0.001164	0.000855
6277	0.000350	0.000479	0.000490	0.000617	0.000654	0.000748	0.000990	0.001178	0.001407
6692	0.000214	0.000265		0.000414	0.000420		0.000561	0.000688	0.000729
7287	0.000366	0.000402	0.000452	0.000553	0.000507	0.000823	0.000826	0.001157	0.001353
8129	0.000328	0.000448	0.000409	0.000509	0.000419	0.000672	0.000962	0.000893	0.000983
9805	0.000327	0.000369	0.000380	0.000450	0.000370	0.000566	0.000748	0.000935	0.001062
Δ	0.000347	0.000433	0.000390	0.000495	0.000453	0.000667	0.000854	0.001055	0.001019
σ	0.000134	0.000183	0.000065	0.000075	0.000068	0.000108	0.000181	0.000193	0.000329

TABLE VI

Skewness normalized to $\bar{\Delta}$ during irradiation

Accumulated Irradiation Time (Hr) / Energy (keV)	3480	433	390	496	453	668	854	1055	1019	Mean
1732	0.93	2.05		1.12	1.15		1.38	1.02	0.67	1.19
2508	1.57	1.32	0.95	0.85		0.95	1.10	1.14	0.63	1.07
2653	0.40	0.73	0.41	0.88	1.11	0.70	0.73	0.76	0.65	0.71
3486	1.51	0.89	1.11	0.82	0.82	1.05	0.95	1.18	1.37	1.08
5299	1.44	1.03	1.06	1.18		0.96	1.17	1.20	1.42	1.18
5373	0.57	0.45	1.03	1.03	0.93	1.15	0.89	1.10	0.84	0.89
6277	1.01	1.11	1.26	1.24	1.44	1.12	1.16	1.12	1.38	1.20
6692	0.61	0.61		0.83	0.93		0.66	0.65	0.72	0.72
7287	1.05	0.93	1.16	1.11	1.12	1.23	0.97	1.10	1.33	1.11
8129	0.94	1.03	1.05	1.03	1.48	1.01	1.13	0.85	0.96	1.05
9805	0.94	0.85	0.97	0.91	1.25	0.85	0.88	0.89	1.04	0.95

Av = 1.01

FIGURE 17

Average skewness measured at different times during irradiation.

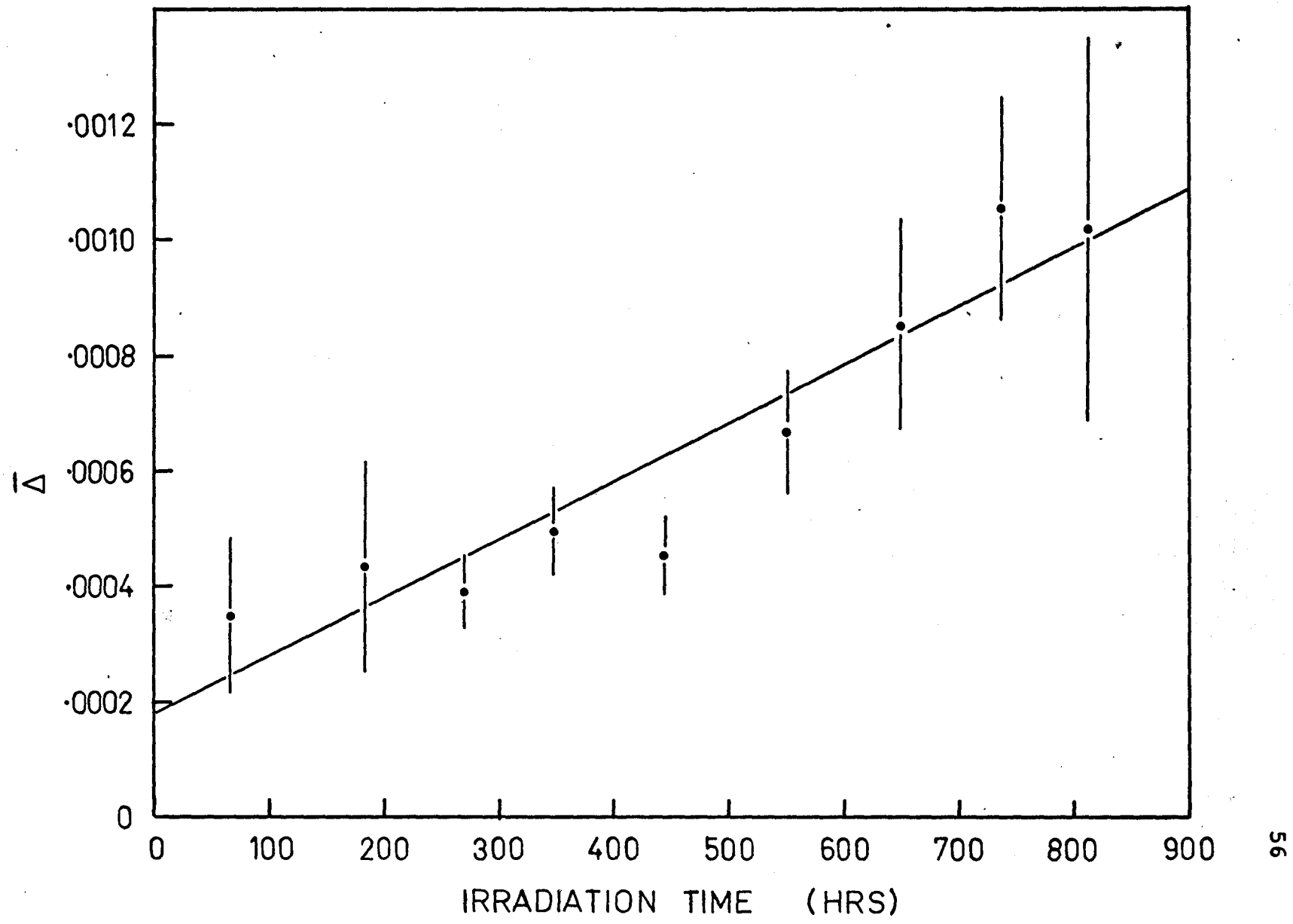
·0012
·0010
·0008
·0006
·0004
·0002
0
|Δ
0
100
200
300
400
500
600
700
800
900
IRRADIATION TIME (HRS)

FIG. 17

time. A least squares fit to this data provided the linear function:

$$\Delta = 1.01 \times 10^{-6} t + 1.80 \times 10^{-4} \qquad (30)$$

where t is measured in hours.

To express this relationship in terms of the total number of neutrons absorbed by the germanium, the slope is divided by the flux rated per hour giving:

$$\Delta = 1.46 \times 10^{-13} I + 1.80 \times 10^{-4} \qquad (31)$$

where $I = \phi t$, $\phi = .7 \times 10^{7}$ neutrons/hr.

This is then substituted into equation (24) in order to obtain for the FWHM of pulse height peaks for this counter:

$$FWHM = 2.35\left(F\varepsilon E + \sigma^2_{elect} + \frac{36}{45}(1.46\times10^{-13} I + 1.80\times10^{-4})^2 E^2\right)^{\frac{1}{2}} \qquad (32)$$

Assume that the Fano factor was the same value as the planar counter A described earlier and that $\sigma_{elect}=1.5$ as before. Then this expression becomes:

$$FWHM = 2.35\left(1.50\times10^{-3} E + 2.25 + .80(1.46\times10^{-13} I + 1.80\times10^{-4})^2 E^2\right)^{\frac{1}{2}} \qquad (33)$$

(where E is expressed in keV).

The effect of increasing irradiation on resolution is shown by the plot of this relationship for gamma rays having energies of 1.0 MeV., 5.0 MeV, and 10.0 MeV in Figure (18).

FIGURE 18

Variation of FWHM of single open ended co-axial detector and analyzing system during irradiation for different gamma ray energies.

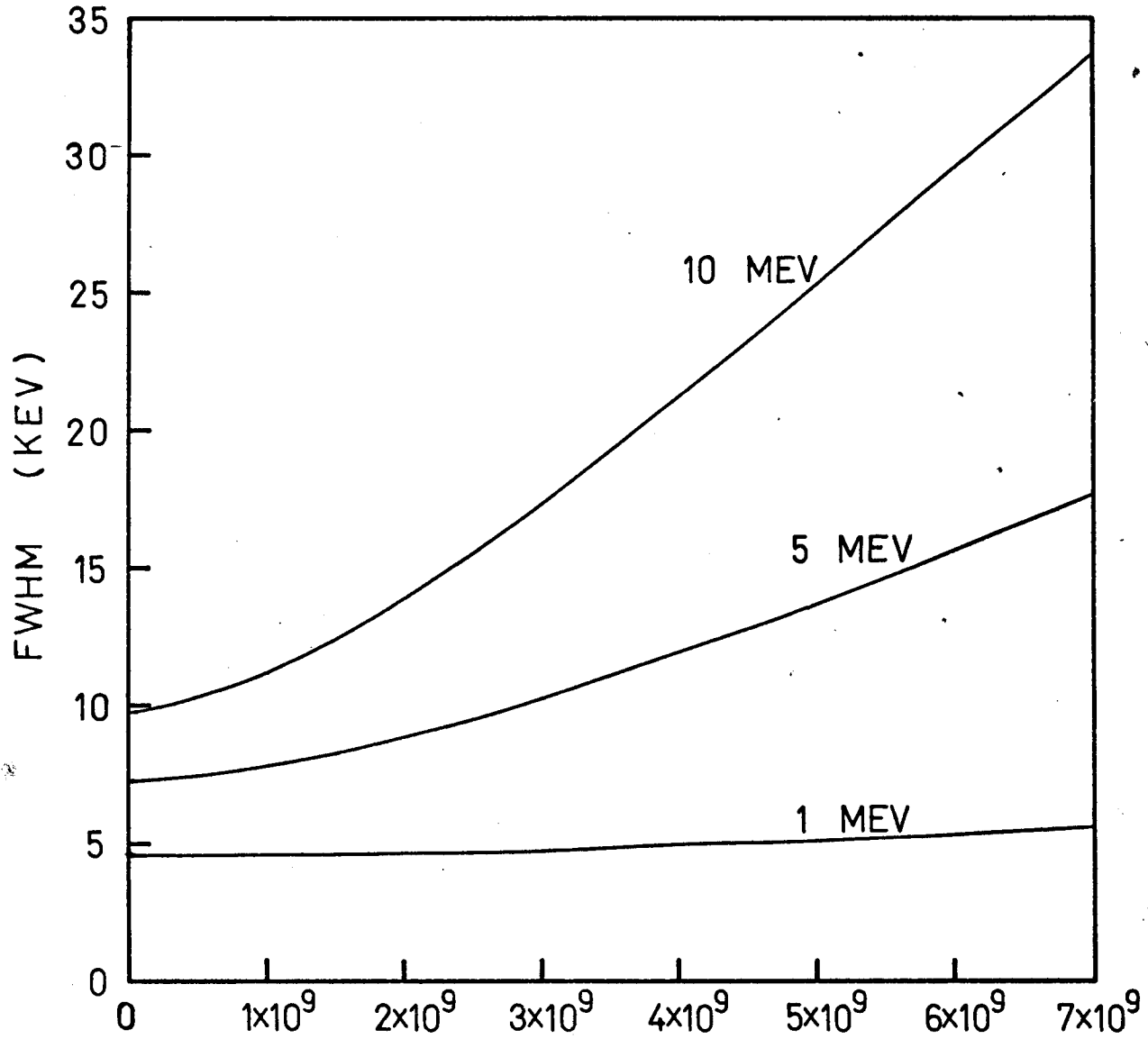
35
30
25
20
15
10
5
0
FWHM (KEV)
10 MEV
5 MEV
1 MEV
0
1x10^9
2x10^9
3x10^9
4x10^9
5x10^9
6x10^9
7x10^9
INCIDENT NEUTRONS

FIG. 18

4.4 Summary

The value of the results in the series of experiments that were described here would be enhanced if there could be found an underlying factor that summarizes the parameters established for each counter. Two obvious relationships lie in the linearity between, first, β and integrated neutron flux and second, the number of defects correlated with the carrier lifetime.

In considering the linearity between β and integrated neutron flux, the results were not conclusive, but a number of points are worth mentioning. Concerning the planar counter A, it appears that a good linear relationship holds between the skewness Δ and increasing neutron does. This would be strengthened however, if a more extensive range of gamma ray energies were used in determining each average Δ. The planar counter B had only two points on which to base a linear function. As such a linear approximation could only be established a priori without being verified. The results for the five sided coaxial counter were complicated by the fact that the electric field across the intrinsic region was not constant. For areas of high electric field, the charge carrier velocities may reach saturation levels so that the low velocity of carriers in low field areas would not necessarily be compensated to an average value which is accurately approximated by a linear

field. This effect would be exaggerated for increased amounts of trapping so that an upswing in the skew against irradiation time graph may result. A second complicating factor was that toward the end of the actual experiment moisture problems necessitated the reduction of the applied bias voltage. This would also aggravate the amount of skewness present in the pulse height peaks and hence cause an upswing in the graph. Both of these factors were possibly present in this experiment.

Therefore one could conclude with certain reservation that a linear relationship exists between skewness and total neutron dose or an inverse relationship between carrier lifetime and total neutron dosage. Any variations that occurred from this were accomplished by complicating factors that could have accounted for difference.

In consideration of the correlation of results between the different counters used, the number of defects required to produce a given amount of skewness could be dealt with. It was noted that with the planar counter A, an increase of 3.5×10^{11} defects/cc was accompanied by an increase of 0.00063 in the average skewness. For planar counter B an increase of 0.55×10^{11} defects/cc was accompanied by an increase of 0.00063 in the skewness. Thus the ratio of the density of defects in counter A to that in counter B was

6.4 while the ratio of the change of skewness in counter A to that in counter B was 5.2. The difference between the two ratios is only 23%. The uncertainty in the volume of the counters would account for about 15% of this error. Thus it can be seen that there is a good correlation in the results from the two Ge(Li) detectors fabricated from germanium that originated from two entirely different sources. A similar correlation would not be obtained for the five sided coaxial detector because it was not possible to determine the colume over which irradiation occurred.

REFERENCES

1. C. Chasman, K. W. Jones and R. A. Ristinen, Nucl. Instr. h. 37 (1965) 1.
2. H. W. Kraner, C. Chasman and K. W. Jones, Nucl. Instr. 2 (1968) 173.
3. H. J. Fiedler, L. B. Hughes, T. J. Kennett, W. V. Prestwich, B. J. Wall, Nucl. Instr. and Meth. 40 (1966) 229.
4. W. Antman, D. A. Landis and R. H. Pehl, Nucl. Instr. 40 (1966) 272.
5. R. Zullinger, D. W. Aitkin, IEEE Trans. Nucl. Sci. 3, 187.
6. Webb, H. L. Malm, M. G. Chartrand, R. M. Green, E. Sakai G. Fowler, Nucl. Instr. and Meth. 63 (1968) 125.
7. L. W. Nichol, A. Lopez, A. Robertson, W. V. Prestwich and T.J. Kennett, Nucl. Instr. and Meth. 81 (1970) 263.